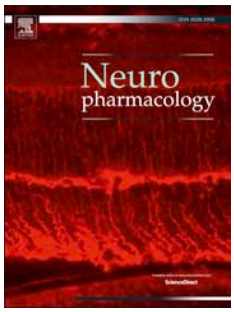

Effects of intranasally-delivered pro-nerve growth factors on the septo-hippocampal system in healthy and diabetic rats

Marzia Soligo, Virginia Protto, Antonio Chiaretti, Sonia Piccinin, Maria Egle De Stefano, Robert Nisticò, Luisa Bracci-Laudiero, Luigi Manni

PII: S0028-3908(20)30291-4

DOI: https://doi.org/10.1016/j.neuropharm.2020.108223

Reference: NP 108223

To appear in: *Neuropharmacology*

Received Date: 1 April 2020

Revised Date: 22 June 2020

Accepted Date: 25 June 2020

Please cite this article as: Soligo, M., Protto, V., Chiaretti, A., Piccinin, S., De Stefano, M.E., Nisticò, R., Bracci-Laudiero, L., Manni, L., Effects of intranasally-delivered pro-nerve growth factors on the septo-hippocampal system in healthy and diabetic rats, *Neuropharmacology* (2020), doi: https://doi.org/10.1016/j.neuropharm.2020.108223.

Effects of intranasally-delivered pro-nerve growth factors on the septo-hippocampal system in healthy and diabetic rats

Marzia Soligo[1], Virginia Protto[1], Antonio Chiaretti[2], Sonia Piccinin[3], Maria Egle De Stefano[4], Robert Nisticò[3,5], Luisa Bracci-Laudiero[1,6], Luigi Manni[1].

CRediT author statement

Marzia Soligo: Conceptualization, Methodology, Investigation, Formal analysis, Writing - Original Draft, Writing - Review & Editing, Visualization. **Virginia Protto:** Investigation, Formal analysis. **Antonio Chiaretti**: Resources. **Sonia Piccinin:** Investigation, Formal analysis, Visualization. **Maria Egle De Stefano**: Writing - Review & Editing, Formal analysis. **Robert Nisticò:** Validation, Writing - Review & Editing, Formal analysis. **Luisa Bracci-Laudiero:** Resources, Writing - Review & Editing. **Luigi Manni**: Conceptualization, Methodology, Investigation, Formal analysis, Writing - Original Draft, Writing - Review & Editing, Project administration.

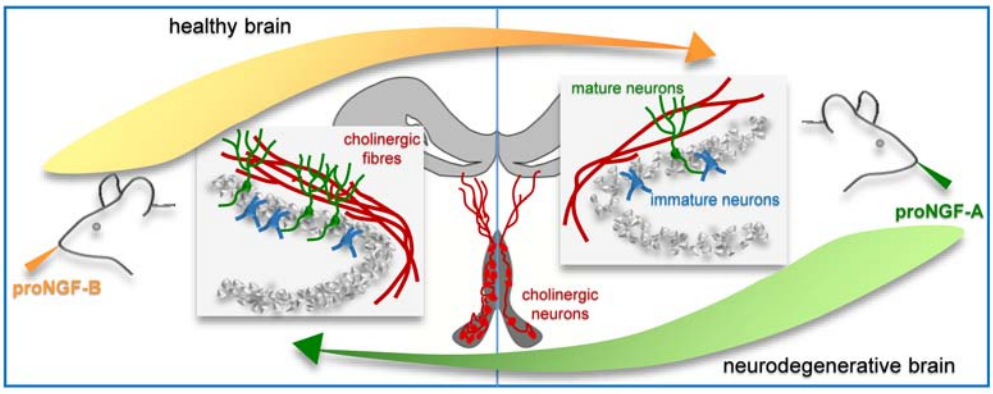

Effects of intranasally-delivered pro-nerve growth factors on the septo-hippocampal system in healthy and diabetic rats

Marzia Soligo[1], Virginia Protto[1], Antonio Chiaretti[2], Sonia Piccinin[3], Maria Egle De Stefano[4], Robert Nisticò[3,5], Luisa Bracci-Laudiero[1,6], Luigi Manni[1].

[1] *Institute of Translational Pharmacology, Consiglio Nazionale Delle Ricerche (CNR), Rome, Italy*

[2] *Institute of Pediatrics, Università Cattolica del Sacro Cuore, Rome – Italy*

[3] *European Brain Research Institute (EBRI), Rome, Italy*

[4] *Department of Biology and Biotechnology "Charles Darwin", Sapienza University, Rome, Italy*

[5] *Department of Biology, University of Rome Tor Vergata, Rome, Italy*

[6] *Division of Rheumatology and Immuno-Rheumatology Research Laboratories, Bambino Gesù Children's Hospital, Rome, Italy*

Corresponding author:

Luigi Manni, Ph.D.
Institute of Translational Pharmacology
National Research Council of Italy (CNR)
via del Fosso del Cavaliere 100
00133, Rome, ITALY
Tel: +39 06 49934248
luigi.manni@ift.cnt.it

Abstract

Pro-nerve growth factor (proNGF) is the predominant form of NGF in the brain and its levels increase in neurodegenerative diseases. The balance between NGF receptors may explain the contradictory biological activities of proNGF. However, the specific role of the two main proNGF variants is mostly unexplored. proNGF-A is prevalently expressed in healthy brain, while proNGF-B content increases in the neuro-degenerating brain. Recently we have investigated *in vitro* the biological action of native mouse proNGF variants. To gain further insights into the specific functions of the two proNGFs, here we intranasally delivered mouse-derived proNGF-A and proNGF-B to the brain parenchyma of healthy and diabetic rats, the latter characterized by dysfunction in spatial learning and memory, in the septo-hippocampal circuitry and by relative increase in proNGF-B hippocampal levels. Exogenous proNGF-B induces depression of hippocampal DG-LTP and impairment of hippocampal neurogenesis in healthy animals, with concomitant decrease in basal forebrain cholinergic neurons and cholinergic fibers projecting to the hippocampus. proNGF-A, while ineffective in healthy animals, rescues the diabetes-induced impairment in DG-LTP and hippocampal neurogenesis, promoting the concomitant recovery of the basal forebrain cholinergic phenotype. Our experimental evidences suggest that the balance between different proNGFs may influence the development and progression of neurodegenerative diseases.

Keywords

pro nerve growth factor (proNGF); hippocampal neurogenesis; dentate-gyrus long-term potentiation (DG-LTP); cholinergic system; diabetes; rat

Abbreviations

NGF- nerve growth factor; mNGF – mature nerve growth factor; proNGF - pro-nerve growth factor; TrkA - Tropomyosin Receptor Kinase A; $p75^{NTR}$ - p75 neurotrophin receptor; DE - diabetic encephalopathy; AD - Alzheimer's disease; DG-LTP – dentate gyrus long-term potentiation; SMG - submaxillary glands; STZ – streptozotocin; BFCN - basal forebrain cholinergic neurons; ChAT - choline acetyl transferase;

1. Introduction

The nerve growth factor (NGF) is a neurotrophin essential for the survival and functional maintenance of developing and adult brain cholinergic neurons (Hefti et al., 1984). In the last two decades the NGF precursor (proNGF) has been described as the prevalent form of NGF detectable in biological tissues (Fahnestock et al., 2001) and its physiological role has been deeply investigated (Hempstead, 2014). Challenging the p75 neurotrophin receptor ($p75^{NTR}$)-sortilin complex, proNGF acts as a pro-apoptotic factor (Nykjaer et al., 2004). By recruiting $p75^{NTR}$ or tropomyosin receptor tyrosine kinase A (TrkA), proNGF induces pro-survival and/or differentiative effects (Fahnestock and Shekari, 2019; Hempstead, 2014; Masoudi et al., 2009; Soligo et al., 2019). Alteration in mature NGF (mNGF)/proNGF processing and proNGF accumulation seem to affect the progression of neurodegeneration in diseases like diabetic encephalopathy (DE) (Soligo et al., 2015) or Alzheimer's disease (AD) (Cuello et al., 2010; Fahnestock et al., 2001). Notably, in experimental model of DE, the specific accumulation of proNGF-B correlated with the development of septo-hippocampal dysfunction (Protto et al., 2019).

Several forms of proNGF were identified in tissue samples from brain and peripheral field (Bierl et al., 2005; Bierl and Isaacson, 2007), suggesting the presence of both splicing variants (Edwards et al., 1986) and/or different levels of glycosylation (Seidah et al., 1996). However, some relevant issues are not yet clarified in the molecular biology of NGF. Among others, the functional significance of the proNGF splicing variants and whether the different proNGF forms influence the development and progression of neurodegenerative diseases. We have recently demonstrated, in PC12 cells that stimulation with purified, mice-derived, native proNGF-A and proNGF-B could elicit different and specific biological responses mediated by different NGF receptors (Soligo et al., 2019).

Aim of the present work was to gain further insights into the specific functions of different proNGF species, both in physiological conditions and during brain neurodegeneration in rats. To achieve this goal, we purified native proNGF-A and proNGF-B from mouse submandibular glands (Soligo et al., 2019) and studied the effects of the two proNGF protein variants, intranasally delivered to the brain parenchyma (Frey et al., 1997; Thorne and Frey, 2001) of healthy and diabetic rats, the latter affected by early signs of brain cholinergic neurodegeneration (Rocco et al., 2013; Soligo et al., 2017). We analyzed the effects of proNGFs on specific hippocampal functions, such as long-term potentiation (LTP) and neurogenesis, known to be regulated by the cholinergic drive from the medial septum (Teles-Grilo Ruivo and Mellor, 2013; Van der Borght et al., 2005).

2. Methods

2.1 Animals

Sixty-day old female Sprague–Dawley rats were purchased from Harlan (Nossan, Italy). Rats were weighed (200–220 g) and housed three per cage, with standard food and water available ad libitum. The animal room had a controlled 12-hours light cycle (lights on at 07:00h), lux level (on average 100 lux), temperature (21±1°C) and relative humidity (50±5 %). All experiments were conducted according to the ARRIVE guidelines (Kilkenny et al., 2010). Animal care procedures were conducted in conformity with the Legislation for the protection of animals used for scientific purposes provided by the relevant Italian law and European Union Directive (Italian Legislative Decree 26/2014 and 2010/63/EU) and the International Guiding Principles for Biomedical Research involving animals (Council for the International Organizations of Medical Sciences, Geneva, CH). Animals were subjected to experimental protocols approved by the Veterinary Department of the Italian Ministry of Health (Permit Number: 192/2015–PR). All adequate measures were taken to minimize animal pain or discomfort and all surgery was performed under isoflurane anesthesia.

2.2 Diabetes induction, *Bromodeoxyuridine administration and proNGFs delivery*

In the present study, a widely accepted animal model of streptozotocin-induced type 1 diabetes was used (Wilson and Leiter, 1990). Streptozotocin (STZ, cat. S0130, Sigma-Aldrich) is selectively toxic to the insulin-producing cells of the pancreas (Wilson and Leiter, 1990). Rats early develop characteristic mild cognitive impairment, associated with neuronal sufferance (Soligo et al., 2017) and dysregulation in the metabolism of protein markers of neurodegeneration, as protein tau and the NGF molecular system (Protto et al., 2019; Rocco et al., 2013). Diabetes was induced in young female rats, as previously described (Protto et al., 2019; Rocco et al., 2013; Soligo et al., 2017), by a single

intraperitoneal injection of 65 mg/kg STZ dissolved in citrate buffer, pH 4.5 (for the experimental plan see Figure S1A). Ninety-six rats were divided in two groups as follow: 48 healthy rats were injected once I.P. with 20 mmol/l citrate, pH 4.5 (healthy groups) and 48 rats were injected with STZ as described above (diabetic groups) (Figure S1A-B). One week after STZ-treatment, the establishment of diabetes was checked with Accutrend™ GC (Roche Diagnostic, Germany) glucose analyzer 3 and allocated rats with glucose levels above 300 mg/dl to the diabetic groups (Figure S1C). Four weeks after STZ-treatment, rats were euthanized and whole brain collected for immediate analysis. To study neuronal differentiation and survival during diabetes development, 12 healthy and 12 diabetic animals we injected with 75 mg/kg of 5-bromo-2′-deoxyuridine (BrdU, cat B5002; Sigma Aldrich) dissolved in saline (10 mg/ml). BrdU was injected daily for 5 days starting 2 days after the induction of diabetes (Figure S1A-B). Four days before euthanasia, healthy and diabetic rats, treated or not with BrdU, were exposed to intranasal administrations of purified proNGF-A, proNGF-B or saline, once a day for four days (Figure S1A-B). Intranasal administration is a non-invasive method of delivering therapeutic agents to the central nervous system along both the olfactory and trigeminal neural pathways (Thorne and Frey, 2001), also tested in human NGF clinical trials (Chiaretti et al., 2017). Awake rats were grasped gently and the head elevated to keep the nasal cavity upward. Five microliters of drug was delivered to each nostril using a micropipette and, after the final droplet, the rat's nose was kept pointing upward for 20 seconds (Dhuria et al., 2010). Each rat received one round of 15 µg of nasal administration per day (in the morning) and was treated for four consecutive days (total amount of drug: 60 µg per rat).

2.3 proNGF purification from mice SMG

Native proNGFs protein variant have been purified from mice submaxillary glands (SMG) as previously described (Soligo et al., 2019). Briefly, SMG homogenate was processed through sequential anion exchange, hydrophobic interaction and size exclusion

chromatographic steps, allowing respectively the isolation of proNGF from crude extract, the discrimination of the two proNGF variant and the final separation of the two proNGF from proteins known to interact with the mature portion of the molecule (Soligo et al., 2019). The analysis of purified fractions, performed by Coomassie staining, Western blot, lectin blotting and nano liquid chromatography-electrospray-tandem mass spectrometry (nLC-ESI-MS/MS), confirmed the successful purification of native proNGF-A and proNGF-B (Soligo et al., 2019).

2.4 mNGF/proNGF ELISA

Total content of proNGF (proNGF-A plus proNGF-B) or mNGF were measured in homogenates from hippocampi by specific ELISAs, as described previously (Soligo et al., 2015) and expressed as pg/mg of total proteins.

2.5 RNA extraction and real time PCR

Total RNA was extracted using TRIzol reagent (Invitrogen) following manufacturer's instruction. Concentrations and purity were evaluated by spectrophotometer. Only samples with λ260/λ280 ratio >1.8 were included in the study. One µg mRNA/sample was used for the cDNA synthesis using the QuantiTect Reverse Transcription kit (Quiagen). proNgf-A (custom Applied Biosystem assay AP322XX) and proNgf-B (custom Applied Biosystem assay AP47WHV) expression levels were measured by real-time PCR. Applied Biosystems assay-on-demand was used to measure β–actin (housekeeping control; cat. Rn4352660). Relative quantification was performed using the comparative Ct method and results were expressed as $2^{-\Delta\Delta Ct}$.

2.6 Electrophysiology

For extracellular recordings, hippocampal slices (350 µM thick) from 8 rats for each experimental group (Fig. S1A-B) were kept submerged at 30°C and superfused (2–3 ml/min^{-1}) with oxygenated (95% O_2, 5% CO_2) artificial CSF. Stimulation was applied to the

medial perforant pathway of the dentate gyrus (DG), using a bipolar insulated tungsten wire electrode, and field excitatory postsynaptic potentials were recorded at a control test frequency of 0.033 Hz from the middle one-third of the molecular layer of the DG with a glass microelectrode. LTP was evoked by high-frequency stimulation (HFS) consisting of eight trains, each of eight stimuli at 200 Hz, and an inter-train interval of two seconds, with the stimulation voltage increased during the HFS protocol. Measurements of LTP were made 60 minutes post-HFS. All solutions contained 50 µM picrotoxin (P1675, Sigma-Aldrich) to block GABA-A-mediated activity.

2.7 Immunofluorescence, Stereology and Confocal Microscopy.

Free-floating coronal brain sections (40 µm-thick) were pre-incubated with PBS containing 10 % (v/v) donkey serum, 1% (w/v) BSA and 0.3% (v/v) Triton X-100, for 2 hours at room temperature (RT). Sections were then incubated with primary antibodies diluted in the same medium (Table S1), overnight at 4°C. Sections were rinsed in PBS and specific secondary antibodies were incubated 2 hours at RT. For double labeling with BrdU, after the immunofluorescence of the antigen of interests, sections were incubated with 2N HCl for 30 minutes at 37 °C and then washed twice with 0.1 M Sodium Borate pH 8.5. BrdU labeling was performed as described above. After extensive washes with PBS, sections were incubated for 10 minutes with Hoechst reagent for nuclei staining.

Coronal brain sections from 3-4 rats/group were processed for confocal microscopy. In preparation for an unbiased estimate of cell numbers, an initial tissue section was selected randomly at one anatomic border of the brain region to be estimated. For hippocampus, the region that spanned from -2.40/-3.72 mm relative to Bregma was analyzed according to Paxinos' Rat Brain atlas (Paxinos, 1982), corresponding to the septal hippocampus. To cover this region of interest, stained slices for each rat were analyzed spacing 320 µm from each other. For medial septum, all the anatomic region that spanned from +1.2/+0.24

mm relative to Bregma was analyzed, processing 1 section every 120 µm. At least four sections were analyzed for each animal in every analysis performed. Stained sections were imaged with a confocal laser-scanning microscope (Leica SP5, Leica Microsystems, Wetzlar, Germany) under sequential mode, to avoid crosstalk between channels. Confocal image acquisition was conducted so that all samples were imaged using consistent settings for laser power and detector gain. Boundaries and subdivisions of the brain structures were identified with reference to the Paxinos' Rat Brain Atlas (Paxinos, 1982). Image analysis was performed by the Imaris Suite 7.4 software (Bitplane A.G., Zurich, Switzerland).

In order to quantify ChAT-positive cells in the medial septum (n=4 rats/group), the number of immunopositive cells was automatically evaluated, using the Imaris Spot module. Cell number obtained for each section was divided for the corresponding area of the section, in order to obtain the average number of cells per square millimeter. The Imaris Surface module was used to automatically draw a mask on ChAT immunostaining and quantify the ChAT immunofluorescence in cells of the medial septum and cholinergic fibers in the fimbria, as previously described (Protto et al., 2019). The obtained masks were used to evaluate the area covered by the ChAT fibers and to measure the mean pixel intensity of ChAT immunostaining.

The total estimated number of Hoechst$^+$, BrdU$^+$, ki67$^+$, DCX and NeuN$^+$ cells within the dentate gyrus in the septal hippocampus (see above) was obtained multiplying the average number of positive cells per section by the total number of sections comprising the region of the dentate gyrus analyzed (about 36 sections) (Protto et al., 2019). Data were expressed as the number of the immune-positive cells on the total number of cells expressing BrdU or ki67 or NeuN in the single hippocampus (n=6-8 hippocampi/group, details in figure captions). For production of figures, processing was done by using the

Adobe Photoshop CS6 software (Adobe Systems Incorporated, San Josè, United States): production, brightness and contrast of images were globally enhanced by using linear histogram correction and images were slightly oversaturated.

2.8 Statistic

Statistical analyses were performed using GraphPad Prism 5 (GraphPad Software). Data are presented as mean ± standard error of the mean (SEM). All analyses were two-tailed and P-values < 0.05 were considered statistically significant. P-values were adjusted for multiple comparisons and reported in figures.

To assess the effect of saline, proNGF-A or proNGF-B (treatment) on healthy or diabetic rats (disease), means were compared by two-way ANOVA and multiple comparisons performed by Bonferroni post-hoc test when main and/or interaction effects were revealed by ANOVA.

3. Results

In the present work, a widely accepted streptozotocin-induced animal model of type 1 diabetes was used (Wilson and Leiter, 1990) in young female rats (Nori et al., 2013; Rocco et al., 2013; Soligo et al., 2015). In this model, the development and progression of diabetes generate mild cognitive impairment and hippocampal-related memory disorder, reducing the functions of the septo-hippocampal cholinergic circuitry and depressing neural plasticity (Soligo et al., 2017). Moreover, diabetic rats early develop mild-to-severe neuronal loss (Soligo et al., 2017) and glial proliferation (Protto et al., 2019).

The rationale for treating diabetic and healthy rats with proNGF-A and proNGF-B, in order to modify the pathological or physiological state respectively, is based on the evidence that experimental diabetic encephalopathy is characterized by increased hippocampal levels of proNGF (Soligo et al., 2015) attributable to specific augment of proNGF-B (Protto et al., 2019). Accordingly, pharmacological treatments were aimed at mimic, in healthy rats, the relative over-abundance of brain proNGF-B observed after diabetes induction (Protto et al., 2019) or at counteracting the latter by exogenously increasing the brain levels of proNGF-A in diabetic rats. To avoid the development of undesired systemic side effects (Dhuria et al., 2010) mouse native proNGF-A and proNGF-B were intranasally delivered in healthy and diabetic rats (Frey et al., 1997; Thorne and Frey, 2001). The timeline of experimental setup and the blood glucose levels are reported in Figure S1A-C. The intranasal delivery of either proNGF-A or proNGF-B did not affect the body weight of healthy rats (Figure S1D) and did not influence the diabetes-induced weight reduction in diabetic rats (Soligo et al., 2017).

3.1 proNGF/mNGF in the hippocampus

To assess if intranasal treatments affected the proNGF and mNGF levels in the hippocampus, the NGF-producing area in the septo-hippocampal circuitry (Whittemore and

Seiger, 1987), specific ELISA, allowing the discrimination between precursor and mature NGF but not between proNGF-A and proNGF-B variants were performed (Figure S2A-C) (Soligo et al., 2015). The already reported increase of proNGF, decrease of mNGF and of mNGF/proNGF protein ratio (Soligo et al., 2015) was confirmed (Figure S2A-C, diabetic *vs* healthy saline-treated rats). Intranasal proNGF-A or proNGF-B in healthy rats decreased hippocampal mNGF and consequently mNGF/proNGF ratio (Figure S2B-C, proNGF-treated *vs* saline-treated healthy rats). Only intranasal proNGF-A decreased hippocampal proNGF levels in diabetic rats, causing a significant increase of mNGF/proNGF ratio (Figure S2A,C, proNGF-A-treated vs saline-treated diabetic rats). The type and extent of the effects observed on NGF protein levels in the hippocampus following intranasal administration of proNGF, indicate that the exogenous proNGFs probably do not reach the hippocampus but indirectly modulate the endogenous production of NGF.

To investigate whether the pharmacological treatments had modulatory effects on the expression of the two variants of proNgf in the hippocampus, specific qPCR assays, which measured the proNgf-A and proNgf-B transcript levels, were performed (Figure S2D-E). proNgf-A-mRNA was decreased, while proNgf-B-mRNA was increased after diabetes induction (Figure S2D-E, healthy vs diabetic saline-treated rats). Both the pharmacological treatments decreased proNgf-A-mRNA and increased proNgf-B-mRNA in healthy rats (Figure S2D-E, proNGF-treated vs saline-treated healthy rats) and did not exert significant effects in diabetic rats (Figure S2D-E).

3.2 Dentate gyrus- long-term potentiation

To explore the possibility that the treatment with proNGFs may alter the excitatory circuits that drive hippocampal functions, influencing dentate gyrus-long term potentiation (DG-LTP), DG-LTP was measured in healthy and diabetic animals treated with intranasal delivery of either saline or proNGF-A or proNGF-B (Figure 1). In healthy rats, the

magnitude of DG-LTP -recorded for 60 minutes after application of HFS to the perforant pathway- was lowered by proNGF-B treatment, while proNGF-A did not induce significant variations when compared with saline-treated rats (Figure 1A). On the contrary, in diabetic rats the administration of proNGF-A fully restored the diabetes-impaired DG-LTP magnitude (Figure 1B) to levels similar to those observed in healthy rats (Figure 1A). The treatment of diabetic rats with proNGF-B did not modify DG-LTP that was not different from the one recorded in saline-treated diabetic animals (Figure 1B).

DG-LTP variation over the baseline during the last 10 minutes of recording (Figure 1C) was analyzed by two-way ANOVA (Figure 1D). The analysis showed that the EPSP was influenced by both diabetes induction and proNGF treatments, with a significant interaction between the two main factors (Figure 1D). Multiple comparisons (values reported in Figure 1C and Figure 1E) confirmed that proNGF-A counteracted the diabetes-induced decrease in DG-LTP magnitude (Figure 1C: proNGF-A-treated *vs* saline-treated diabetic rats and Figure 1E: diabetic *vs* healthy saline-treated rats) almost restoring it at healthy controls level. DG-LTP magnitude in healthy rats was reduced after treatment with proNGF-B (Figure 1C: proNGF-B-treated *vs* saline-treated healthy rats), such as the one recorded in saline-treated diabetic rats. The administration of proNGF-B to diabetic rats did not further modify the decreased DG-LTP magnitude (Figure 1C: proNGF-B-treated *vs* saline-treated diabetic rats, $P>0.05$). These data provide a first indication about the possibility of modulating hippocampal neurophysiology by exogenous proNGF treatment and reveal that different proNGF protein variants exert different effects on hippocampal synaptic plasticity.

3.3 Hippocampal DG cells morphology

To verify whether the observed effects of proNGF-A and proNGF-B on hippocampal neurophysiology were associated with alterations in DG-hilus and DG-granular layer morphology, cell number, nuclear size and $NeuN^+$ cells (Soligo et al., 2017) were analyzed

in healthy and diabetic rats treated with saline, proNGF-A or proNGF-B (Figure 2). Details on two-way ANOVA and multiple comparisons relative to disease development (healthy vs diabetic) are summarized below each graph (Figure 2C-H). Multiple comparisons relative to pharmacological treatments are reported in the graphs.

Significant effects on total cell numbers, induced by either disease and treatment and significant disease x treatment interaction effect, were revealed by two-way ANOVA and observed in both analyzed areas (Figure2C, F). Significant total cell loss in both DG-hilus (Figure 2A) and DG-granular layer (Figure 2B) was observed after induction of diabetes (Figure 2C, F: diabetic *vs* healthy saline-treated rats). In healthy rats, the treatment with proNGF-B induced significant cell loss both in DG-hilus and DG-granular layer (Figure 2C, F: proNGF-B-treated *vs* saline-treated healthy rats), while the treatment with proNGF-A did not affected the number of cells in both areas (Figure 2C, F: proNGF-A-treated *vs* saline-treated healthy rats; $P>0.05$). Neither proNGF-A nor proNGF-B modified the diabetes-induced decrease of total cell number observed in DG-hilus and DG granular layer (Figure 2C, F).

Analysis of the nuclear size revealed significant main effects induced both by the development of disease and proNGF treatments in DG-hilus and DG-granular layer, while significant disease x treatment interaction was observed in the DG-hilus only (Figure 2D, G). Diabetes development induced nuclear enlargement in both analyzed areas (Figure 2D, G: diabetic *vs* healthy saline-treated rats). In healthy rats, proNGF-A treatment reduced nuclear diameters in both analyzed areas (Figure 2D, G: proNGF-A-treated *vs* saline-treated healthy rats), while it counteracted the diabetes-induced nuclear enlargement in the DG-granular layer only (Figure 2G: proNGF-A-treated *vs* saline-treated diabetic rats). proNGF-B treatment neither induced effects in healthy nor in diabetic

animals (Figure 2D, G: proNGF-B-treated *vs* saline-treated healthy and diabetic rats, $P > 0.05$).

To study the effect of intranasally-delivered proNGF-A and proNGF-B on the reported diabetes-induced hippocampal neuronal loss (Soligo et al., 2017), the number of $NeuN^+$ cells were analyzed in DG-hilus and DG-granular layer (Figure 1E, H). Significant effects on the number of $NeuN^+$ cells, induced by treatments in DG-hilus and by disease in DG-granular layer, were revealed by two-way ANOVA and significant interaction effects were observed in both analyzed areas (Figure 2E, H). These effects were further elucidated by multiple comparisons analysis (Figure 2E, H), which confirmed that diabetes establishment induced significant $NeuN^+$ cell loss in both DG-hilus and DG-granular layer (Figure 2E, H: diabetic *vs* healthy saline-treated rats). In healthy animals, proNGF-B treatment decreased the number of $NeuN^+$ cells in both regions (Figure 2E, H: proNGF-B-treated *vs* saline-treated diabetic rats) while proNGF-A did not modify the number of neurons. Moreover, the loss of neurons induced by diabetes was counteracted by proNGF-A treatment in the DG-hilus (Figure 2E: proNGF-A-treated *vs* saline-treated diabetic rats), while proNGF-B did not worsen the observed $NeuN^+$ cell loss (Figure 2E: proNGF-B-treated *vs* saline-treated diabetic rats; $P > 0.05$).

Overall, these data indicate that, while proNGF-B decreased the number of hippocampal cells, when delivered in healthy animals, proNGF-A, normalizing nuclear size in the DG-granular layer and the number of hilar neurons in diabetic rats, may dampen an early and/or adaptive response to neurodegeneration (Riudavets et al., 2007).

3.4 Hippocampal neurogenesis

Hippocampal neurogenesis sustains hippocampal plasticity (Snyder et al., 2001) being in turn regulated by the latter (Bruel-Jungerman et al., 2006). In addition, neurogenesis is positively affected by mNGF (Frielingsdorf et al., 2007), while proNGF is thought to elicit

an inhibitory action on adult mice neurogenesis (Guo et al., 2013). The summary of two-way ANOVA analyses on hippocampal neurogenesis, in relation to diabetes induction and proNGF treatments, and multiple comparisons relative to disease development (healthy vs diabetic) are summarized below each graph. Multiple comparisons relative to pharmacological treatments are reported in the graphs. Significant main effect in both treatment and disease factors and in the disease x treatment interaction were found by ANOVA for the number of $BrdU^+$-incorporating cells in the DG (Figure 3B). Diabetes decreased such cell number in the DG (Figure 3A-B: diabetic *vs* healthy saline-treated rats). A similar effect was observed after proNGF-B treatment in healthy rats (Figure 3A-B: proNGF-B-treated *vs* saline-treated healthy rats). proNGF-B, however, did not worsen the diabetes-induced decrease in $BrdU^+$-incorporating cells. proNGF-A did not affect the number of $BrdU^+$ cells in healthy rats (Figure 3A-B: proNGF-A-treated *vs* saline-treated healthy rats; $P>0.05$) but when administered to diabetic rats it enhanced the number of $BrdU^+$ cells, restoring it at saline-treated healthy control level (Figure 3A-B: proNGF-A-treated *vs* saline-treated diabetic rats).

To study the progression of the neuronal phenotype in cells incorporating BrdU at the time of diabetes induction (see Figure S1), the number of $BrdU^+$ cells expressing doublecortin (DCX: immature neurons marker) or NeuN (mature neurons marker) were analyzed (Figure 3C). Two-way ANOVA, for $BrdU^+/DCX^+$ returned a significance for the main factor treatment and for the disease x treatment interaction (Figure 3D). The same analysis applied to the number of $BrdU^+/NeuN^+$ cells revealed significant effects for both main factors and for the interaction between them (Figure 3E).

The progression of diabetes did not modify the number of immature $BrdU^+/DCX^+$ neurons (Figure 3D: diabetic *vs* healthy saline-treated rats; $P>0.05$), but induced a significant decrease in the number of $BrdU^+/NeuN^+$ neurons (Figure 3E: diabetic *vs* healthy saline-

treated rats). proNGF-B significantly reduced both immature and mature newborn neurons in healthy animals (Figure 3D-E: proNGF-B-treated *vs* saline-treated healthy rats), while it did not modify the number of both immature and mature newborn neurons in diabetic rats (Figure 3D-E: proNGF-B-treated *vs* saline-treated diabetic rats; $P>0.05$). Exogenous proNGF-A had no effects on healthy rats but rescued the diabetes-impaired number of mature newborn neurons, improving it at the level found in saline-treated healthy rats (Figure 3D-E: proNGF-A-treated *vs* saline-treated diabetic rats). These results suggest that exogenous proNGF-B may interfere with the physiological process of neurogenesis, affecting the number of immature and mature neurons that incorporated BrdU, but it does not influence the diabetes-induced dysfunction in the generation of new neurons. Conversely, exogenous proNGF-A does not affect physiological neurogenesis while it may promote neural development and differentiation up to the mature final stage in diabetic brain.

The number of actively proliferating cells at the time of sacrifice (Figure 4), evaluated by counting ki67-immunopositive cells, was affected by pharmacological treatments, with significant interaction between the two factors analyzed by two-way ANOVA (Figure 4B). The number of $ki67^+$ cells in the DG increased significantly in diabetic compared to healthy rats (Figure 4A-B: diabetic *vs* healthy saline-treated rats). The proNGF-B delivery significantly decreased the number of $ki67^+$ cells in the DG of healthy rats (Figure 4B: proNGF-B-treated *vs* saline-treated healthy rats). A similar reduction was also observed in diabetic rats treated with either proNGF-A or proNGF-B (Figure 4B: proNGF-A- or proNGF-B-treated *vs* saline-treated diabetic rats).

To further investigate this aspect, the proliferation rate of DCX-expressing immature neurons, which are known to exhibit proliferative activity (Kempermann et al., 2004), were selectively analyzed (Figure 4C-D). The number of $DCX^+/Ki67^+$ double immunopositive

neurons was affected by disease and treatment, without significant disease x treatment interaction, as shown in the ANOVA (Figure 4D). Such number decreased in diabetic compared to healthy rats (Figure 4D: diabetic *vs* healthy saline-treated rats), suggesting that the increase in the total number of $ki67^+$ cells observed after diabetes induction (Figure 4A-B) could be ascribed to non-neuronal lineage proliferation. Significant reduction in the number of $DCX^+/ki67^+$ cells was found in healthy rats treated with proNGF-B (Figure 4D: proNGF-B-treated *vs* saline-treated healthy rats). Conversely, proNGF-A treatment ameliorated the diabetes-induced decrease in the proliferation rate of neuronal precursors (Figure 4D: proNGF-A-treated *vs* saline-treated diabetic rats), improving it at levels comparable to those of saline-treated healthy rats. These evidences suggest that proNGF-A is effective in sustaining the proliferation of cells committed to neuronal phenotype, in diabetic animals.

3.5 Basal forebrain cholinergic system

The cholinergic drive from basal forebrain cholinergic neurons (BFCN) positively affects adult hippocampal neurogenesis (Mohapel et al., 2005; Van der Borght et al., 2005) and modulate hippocampal plasticity and DG-LTP (Teles-Grilo Ruivo and Mellor, 2013). To studied whether the delivery of proNGFs to the brain could modulate the diabetes-impaired cholinergic phenotype and neurotransmission (Soligo et al., 2017), the number of medial septum total and cholinergic neurons and the choline acetyl transferase (ChAT) content were analyzed, in both cholinergic neurons (Figure 5) and fimbria fibers (Figure 6).

Details on two-way ANOVA and multiple comparisons relative to disease development (healthy vs diabetic) are summarized below each graph (Figure 5-6). Multiple comparisons relative to pharmacological treatments are reported in the graphs. No significant effects in two-way ANOVA were found analyzing the total neurons of medial septum while significant effects were present examining ChAT cell number and fluorescence intensity for both the

factors and for their interaction (Figure 5B, D-E). The graphical sketches in Figure 5A and 6A represent the cholinergic neurons, the fimbria fibers conveying ChAT enzyme from the basal forebrain to the hippocampus and the areas analyzed.

The onset of diabetes did not modify the number of total neurons in the medial septum (Figure 5B) but selectively decreased the number of $ChAT^+$ neurons (Figure 5C-D: diabetic *vs* healthy saline-treated rats). The ChAT content -measured as pixel mean fluorescence intensity- was also significantly reduced in $ChAT^+$ neurons of diabetic rats (Figure 5E: diabetic *vs* healthy saline-treated rats). In healthy animals, proNGF-B treatment did not affect the number of total neuron (Figure 5B, proNGF-B-treated *vs* saline-treated healthy animals; $P>0.05$). Conversely, proNGF-B selectively decreased the number of neurons expressing ChAT (Figure 5C-D: proNGF-B-treated *vs* saline-treated healthy rats) without altering the ChAT content in the neurons that still express ChAT (Figure 5E: proNGF-B-treated *vs* saline-treated healthy rats; $P>0.05$). No significant effects were measured in diabetic rats treated with proNGF-B (Figure 5C-E: proNGF-B-treated *vs* saline-treated diabetic rats; $P>0.05$). Conversely, proNGF-A treatment selectively ameliorated the diabetes-induced decrease in $ChAT^+$ neurons (Figure 5C-D: proNGF-A-treated *vs* saline-treated diabetic rat) and their ChAT pixel intensity (Figure 5E: proNGF-A-treated *vs* saline-treated diabetic rat), while did not affect these parameters in healthy animals (Figure 5C-E: proNGF-A-treated *vs* saline-treated healthy rats). These data indicate that the two proNGF protein variants differently affect the cholinergic neurons phenotype in the medial septum without altering the total number of neurons in the same area.

To study the ability of cholinergic neurons to reach hippocampus, $ChAT^+$ fibers in the fimbria were analyzed, both in a region proximal to the medial septum and at the hippocampal level (Figure 6A). In diabetic animals, the percentage of area occupied by $ChAT^+$ fibers decreased both in the region proximal to medial septum (Figure 6B-C:

diabetic *vs* healthy saline-treated rats) and in the area close to the hippocampus (Figure 6E-F: diabetic *vs* healthy saline-treated rats). In both regions, ChAT fluorescence intensity within fimbria fibers was not modified by diabetes induction (Figure 6D, G: diabetic *vs* healthy saline-treated rats; $P>0.05$), indicating that the remaining fibers are able to convey a proper amount-per-fiber of the enzyme to their terminals. In healthy animals, proNGF-B delivery decreased the amount of $ChAT^+$ fibers in both regions (Figure 6C, F: proNGF-B-treated *vs* saline-treated healthy rats), while proNGF-A restored the diabetes-induced loss of $ChAT^+$ fibers (Figure 6C, F: proNGF-A-treated *vs* saline-treated, diabetic rats). Neither proNGF-B nor proNGF-A modified the $ChAT^+$ fibers fluorescence intensity (Figure 6D, G). Overall, these data indicate that increased brain proNGF-B may interfere with the survival and/or the phenotypic maintenance of cholinergic neurons, while proNGF-A may rescue the cholinergic phenotype in neurodegenerative conditions.

4. Discussion

The data presented in the current work indicate that purified native mouse proNGFs intranasally delivered to the brain parenchyma (Frey et al., 1997; Thorne and Frey, 2001) can differentially affect the brain septo-hippocampal system both in healthy rats and in rats affected by early diabetic encephalopathy. The existence of different proNgf transcripts in mouse tissues (Edwards et al., 1986) and their relative tissue abundance (Selby et al., 1987) has been reported since decades. Despite these evidences and the detection of at least two main different protein variants in both mouse and rat tissues (Bierl et al., 2005; Bierl and Isaacson, 2007; Soligo et al., 2015) the possible differential activity of the long (proNGF-A) and short (proNGF-B) precursor forms of NGF has been poorly addressed. It has been recently demonstrated that the physiological equilibrium of the two main proNGF protein variants is altered in a model of early diabetic encephalopathy, suggesting that the relative increase in proNGF-B in the brain of diabetic rats is linked to the onset and development of neurodegeneration (Protto et al., 2019; Soligo et al., 2015). Moreover, mouse-derived proNGF-A and proNGF-B could elicit different and specific effects on PC12 cells (Soligo et al., 2019).

In the present work, through a combination of electrophysiological, immunohistochemical and morphological analyses it was found that proNGF-B, when intranasally-delivered in healthy rats, triggered the development of neurodegenerative features in the septo-hippocampal circuitry and structures, similar to those currently found and previously described after diabetes induction (Soligo et al., 2017). ProNGF-B depressed hippocampal DG-LTP, impaired hippocampal neurogenesis and decreased both the total number of cells and specifically the number of neurons in hippocampal DG, with a concomitant decrease in the number of basal forebrain neurons expressing the cholinergic marker ChAT and in the number of fibers conveying cholinergic inputs from the medial septum to

the hippocampus. On the other hand, proNGF-A rescued the diabetes-induced impairment of DG-LTP and hippocampal neurogenesis, promoting a concomitant recovery of the basal forebrain cholinergic phenotype, early and severely affected by the development of experimental diabetic encephalopathy (Rocco et al., 2013; Soligo et al., 2017; Welsh and Wecker, 1991). The treatment with proNGF-B did not interfere further with the pathological condition of diabetic rats, probably because of the already established unbalance in proNGF variants, characterized by proNGF-B over-abundance (Protto et al., 2019). Similarly, exogenous proNGF-A did not substantially modify the physiology of the septo-hippocampal circuitry in healthy brain, in which proNGF is represented by the proNGF-A protein variant only (Protto et al., 2019).

The intranasal administration of proNGFs modulated the gene expression and protein content of proNGF in the hippocampus of healthy and diabetic rats. The apparent lack of correlation between the measured trends for RNA and protein can be explained by the possible differences in the specific mechanisms of regulation of gene expression, alternative splicing of mRNAs, their translation into proteins and the subsequent metabolism of these latter. Despite this, the limited extent in the variations of proNGF protein content indicates that intranasally injected neurotrophins probably do not reach, at least in substantial amount, the hippocampus via this route of administration. It was previously reported that intranasally-delivered radiolabeled NGF in rats was mostly traced in the olfactory bulbs and distributed in other brain regions in a decreasing rostro-caudal gradient (Frey et al., 1997). This observation suggests that intranasal proNGFs probably target brain nuclei that, directly or through multi-synaptic pathways, send afferent inputs to the hippocampus. Thus, the observed modulation in proNGFs/mNGF expression and protein content in the hippocampus might be the consequence of an activity-regulated proNGF expression (Thoenen et al., 1991; Zafra et al., 1991) and maturation (Bruno and Cuello, 2006). Nevertheless, the modulation of proNGF-A and proNGF-B content achieved

after intranasal treatments of healthy and diabetic rats seems to be coherent with the observed biological effects and will be discussed below, in a proper correlation with the modulation of DG-LTP, hippocampal neurogenesis and septal cholinergic phenotype.

The intranasal delivery of native murine proNGF variants affects hippocampal synaptic plasticity in both healthy and diabetic rats. It has been reported previously that DG-LTP was impaired (Reisi et al., 2010; Soligo et al., 2017) and the proNGF-B/proNGF-A ratio was concomitantly increased in the hippocampus of diabetic rats (Protto et al., 2019). Notably, the present results indicate that the intranasal delivery of proNGF-B to healthy rats impaired DG-LTP similar to what observed in saline-treated diabetic rats. NGF delivery to the brain of LTP-deficient rats *in vivo* rescued synaptic plasticity through the activation of TrkA (Bergado et al., 1997; Kelly et al., 1998). As far as it turns out, nobody attempted at delivering purified proNGF protein to the brain parenchyma *in vivo*, in order to study its effect on hippocampal plasticity. The rescuing potential of lentiviral-injected proNGF-B transcript on beta-amyloid-induced LTP decline in the rat hippocampus has been reported (Uzakov et al., 2015). Though apparently contrasting with the present results, it is worth noticing that native proNGF-B gene expression in eukaryotic cells almost produces mature NGF, after furin-intracellular processing of proNGF (Masoudi et al., 2009; Pagadala et al., 2006). Thus, it is conceivable that those previously observed (Uzakov et al., 2015) are effects of the mature NGF released by lentiviral-infected hippocampal neurons, while those elicited by nativeexogenous proNGF-B attains to this latter, since it is neither subject to intracellular processing nor prone to rapid degradation in the extracellular milieu (Soligo et al., 2019). At the same time, it cannot be excluded that the LTP-rescuing effects promoted by proNGF-A treatment in diabetic rats may be secondary to the conversion of the exogenous pro-neurotrophin in its mature counterpart, after the intranasal delivery. ELISA data presented here, demonstrating a proNGF-A-induced increase in mNGF/proNGF ratio in the hippocampus of diabetic rats, also indicate

that activity-dependent maturation of hippocampus-produced proNGF (Bruno and Cuello, 2006) is promoted by exogenous proNGF-A, possibly as a consequence of the activation of hippocampal afferents.

Previous data are here confirmed, about the deleterious effects of diabetes on hippocampal LTP (Biessels et al., 1996; Soligo et al., 2017). Furthermore, in this work it was not observed any further impairment of DG-LTP in diabetic rats treated with proNGF-B. It has been recently demonstrated that DG-LTP dysfunctions in this diabetes model might arise from a cholinergic un-responsivity, most probably due to the diabetes-induced functional deficit of muscarinic M1 acetylcholine receptor (Soligo et al., 2017). In the present study this observation was extended, demonstrating that the modulatory cholinergic tone from medial septum to the hippocampus is also impaired in both diabetic rats and in healthy rats treated with proNGF-B. Thus, it could be hypothesized that the lack of a summation effect between diabetes and proNGF-B might possibly be due to the engagement of common biochemical pathways underlying LTP for each of the two conditions. A clue supporting this hypothesis comes from the lack of any further decrease in mNGF/proNGF ratio when proNGF-B treatment was performed on diabetic rats (Figure S2).

The neuronal suffering in diabetic rats is indicated by the observed alterations in hippocampal plasticity. This is supported by the decrease both in the number of total cells and in the number of neurons detected in the dentate gyrus. The number of non-neuronal cells was not analyzed in the present work, which was specifically aimed to investigate the neuronal lineage. Additional experiments will be necessary to disclose the effect of proNGF protein variants treatments on non-neuronal cells, which are known to be incremented in diabetes-induced encephalopathy (Protto et al., 2019). Cell death and neuronal damage in the DG of STZ-treated rodents has been previously described (Can et

al., 2018; Piotrowski et al., 2001; Soligo et al., 2017). Extending these evidences, it was found significant diabetes-induced increase in the volume of cell nuclei in the granular layer of the DG. This was previously interpreted as an early neuronal reaction or a compensatory mechanisms triggered by neurodegenerative insults (Riudavets et al., 2007) and here partially counteracted by proNGF-A treatment. The treatment of healthy rats with proNGF-B seems to be as deleterious as diabetes induction, promoting cell loss in the overall DG and specifically affecting the neuronal phenotype. It is actually not possible to unravel the precise mechanism underlying the neurotoxic effects of exogenous proNGF-B in healthy rats, but it is conceivable that this may depend upon the challenge of $p75^{NTR}$. Previous data about the deleterious effects of proNGF-B interaction with $p75^{NTR}$ (Beattie et al., 2002; Lee et al., 2001) support this hypothesis. This receptor is known to be overexpressed in the septo-hippocampal system after STZ treatment (Protto et al., 2019) as well as in the hippocampi of AD patients (Ito et al., 2016). Notably, the hyper-activation of $p75^{NTR}$ by proNGF has also been proposed as an active neuro-degenerative mechanism in AD (Fahnestock and Shekari, 2019). As for proNGF-A, its effect is more nuanced and once again restricted to diabetic rats, where it promotes the rescue of normal neuro-morphological characteristics. In particular, the recovery of neuronal phenotype in the hilus of DG in STZ-treated rats after intranasal delivery of proNGF-A can have a functional meaning in the recovery of DG synaptic plasticity and in the overall processing of cortical information to DG, considering the crucial role of hilar cells in these hippocampal functions (Wright and Jackson, 2014).

The present data on the effects of proNGF-B on adult hippocampal neurogenesis in healthy rats are well in accord with those demonstrating that infusion of cleavage-resistant proNGF-B into hippocampus inhibits neurogenesis, by decreasing $DCX^+/BrdU^+$ cells, inducing DG cell apoptosis and activating resident astrocytes and microglia (Guo et al., 2013). On the other hand, the number of $DCX^+/BrdU^+$-expressing cells in diabetic rats was

not different from that of healthy control rats (Figure 3D). It should be taken into account that DCX is representative of three subpopulation of progenitor cells committed toward the neuronal phenotype: proliferating type 2b and type 3 and post-mitotic neural precursors, the latter co-expressing DCX and NeuN (Kempermann et al., 2004; Knoth et al., 2010). The presently observed diabetes-induced reduction of $DCX^+/ki67^+$ (both type 2b and type 3 proliferating neural precursors) (Knoth et al., 2010) suggest that at least a sub-population of cycling DCX-expressing neural stem cells is vulnerable to the hyperglycaemic insult. The lack of effect of diabetes on the total number of DCX/BrdU-expressing cells (Figure 3D) might thus represent a block of the progression toward the neuronal phenotype, with a relative accumulation of a DCX subpopulation less vulnerable to the effects of hyperglycaemia. This hypothesis is further suggested by the parallel diabetes-induced decrease of the $NeuN^+/BrdU^+$ population (Figure 3E).

ProNGF-A was able to rescue stem cells proliferation and their final maturation into mature neurons in diabetic rats. This may positively affect the recovery of physiological DG-LTP in diabetic animals, since it is known that hippocampal neurogenesis provides support to hippocampal plasticity (Snyder et al., 2001). Moreover, proNGF-A seems to exert a beneficial effect on the possible hyper-proliferation of glial cells in diabetic rats, as suggested by its counteracting action on the increase in $Ki67^+$ cells and the parallel decrease in $DCX^+/Ki67^+$ cells observed in the DG of diabetic rats. These effects were concomitant to the improvement of mNGF/proNGF ratio promoted by proNGF-A delivery to diabetic rats, an evidence deserving further specific investigations, nevertheless suggesting a positive role for proNGF-A intranasal delivery in the control of neuroinflammation, through its modulatory action on hippocampal endogenous mNGF/proNGF metabolism (Zhao et al., 2017). It is worth noting that cleavage-resistant proNGF-B was found mitogenic for hippocampal stem cells (Corvaglia et al., 2019). However, this effect was specifically addressed to the radial glia-like (RGL) subpopulation

of proliferating progenitors not expressing neuronal commitment markers, such as DCX, and still able to differentiate into glial cells. This could account for the reactive gliosis that is often found in many neurodegenerative diseases, also characterized by increased proNGF-B levels in the hippocampus (Protto et al., 2019).

The effects of exogenous proNGFs on the MS cholinergic phenotype was investigated, since a close interaction exists among septo-hippocampal cholinergic drive, DG-LTP and hippocampal neurogenesis, aimed at the regulation of learning and memory processes (Bliss and Collingridge, 1993; Mohapel et al., 2005). Lesions of the basal forebrain cholinergic nuclei (BFCN) impair both hippocampal plasticity (Drever et al., 2011) and neurogenesis (Cooper-Kuhn et al., 2004). The data in the present manuscript suggest that the function of the circuits wiring BFCN and hippocampal nuclei might be influenced by intranasally delivered proNGF protein variants. The effect of exogenous mNGF on BFCN metabolism, the process of learning and memory and hippocampal synaptic plasticity has been deeply investigated (Gibon and Barker, 2017). However, a few studies have addressed the effects of proNGF on these specific brain functions, indicating that proNGF-B induces cholinergic deficit associated with learning and memory impairment (Tiveron et al., 2013). Moreover, the dysfunction of the cholinergic drive here observed in healthy rats treated with exogenous proNGF-B is similar to that observed after the development of experimental diabetes (Rocco et al., 2013; Sherin et al., 2012; Soligo et al., 2017; Welsh and Wecker, 1991), which is also characterized by selective increase in hippocampal proNGF-B protein variant (Protto et al., 2019). Thus, it is conceivable that, contrary to proNGF-A, proNGF-B may participate in the establishment of diabetes-induced impairment of the cholinergic septo-hippocampal modulatory drive. Although beyond the aim of the present work, the direct proNGF delivery to BFCN could be of help in clarifying the link between proNGF-induced MS cholinergic neurons loss and alterations in DG-LTP and neurogenesis.

The treatment with native mouse-derived proNGFs represents at the same time a strength and a flaw of the present study. The use of native proNGFs strengthen the experimental design, representing a physiological approach compared to the treatment with proNGFs derived by prokaryotic expression systems (Pedraza et al., 2005). On the other hand, it is difficult to draw proper pharmacokinetics considerations for such molecules, since their detection by immunoassays might return imprecise outcomes, biased by possible interferences with endogenous proNGF and by the current uncertainty about their processing after intranasal delivery. The data presented in this work seem to exclude a direct interaction between the septo-hippocampal cells and the intranasally delivered drugs, nevertheless suggesting that these treatments might affect the NGF expression and metabolism in the hippocampus. Previous experiments on PC12 cells (Soligo et al., 2019) indicated that, by using native proNGF protein variants, it is likely to obtain valuable information about the different biological role of proNGF-A, proNGF-B and mNGF. This demonstrated that there was no substantial proteolysis of native proNGFs exogenously dispensed to PC12 cells and that they affected NGF gene expression and protein synthesis (Soligo et al., 2019). It is thus conceivable that native proNGF protein variants may well resist to the extracellular proteases-mediated proteolytic processes (M. A. Bruno and Cuello, 2006; Lee et al., 2001) after their delivery to the brain parenchyma remaining sufficiently unaffected to produce specific effects, not attributable to their transformation into mNGF. A careful evaluation of PD/PK features of tagged recombinant proNGFs will be of great help in answering open questions, such as their tissue distribution and clearance after intranasal delivery to the brain and whether different NGF receptors are involved in the observed pharmacological outcomes.

Although beyond the aim of the present study, an appropriate understanding of the pharmacological potential of proNGF-A and proNGF-B cannot be separated from a thorough characterization of the possible difference in NGF receptors activation by the

proNGF variants. Both molecules have the ability to interact with $p75^{NTR}$, but previous data indicate that the biological outcomes elicited by these interactions is different (Soligo et al., 2019). Indeed it has been previously demonstrated that only proNGF-A stimulates $p75^{NTR}$-mediated neuroprotective effects, while, after blocking $p75^{NTR}$ by the selective antagonist LM11A-31, proNGF-B promotes the survival and differentiation of serum-deprived PC12 cells (Soligo et al., 2019). These results suggest that counteracting $p75^{NTR}$ activation may prevent both the proNGF-B-induced and the diabetes-induced deleterious effects on the septo-hippocampal physiology.

4.1 Conclusion

In conclusion, the present in vivo data confirm the previous *in vitro* observations about the different biological activity of proNGF-A and proNGF-B. This leads to hypothesize that the neurotoxic effect to date ascribed to proNGF may be attributed selectively to proNGF-B. Such hypothesis open new translational scenarios, in which proNGF-B/proNGF-A ratio may have a novel value as diagnostic/prognostic biomarker in human diseases characterized by aberrant activation of proNGF signaling, such as Alzheimer's disease (Cuello et al., 2010; Fahnestock et al., 2001; Schliebs and Arendt, 2011), Down Syndrome (Iulita and Cuello, 2015), Traumatic Brain Injuries (Beattie et al., 2002) and several cancer types (Bradshaw et al., 2015).

Acknowledgement:

The authors acknowledge the valuable technical assistance of Sig. Mauro Fabiani (Institute of Translational Pharmacology - CNR).

Funding Source: This research did not receive any specific grant from funding agencies in the public, commercial, or not-for-profit sectors.

Declarations of interest: none

References

Beattie, M.S., Harrington, A.W., Lee, R., Kim, J.Y., Boyce, S.L., Longo, F.M., Bresnahan, J.C., Hempstead, B.L., Yoon, S.O., 2002. ProNGF induces p75-mediated death of oligodendrocytes following spinal cord injury. Neuron 36, 375–86.

Bergado, J.A., Fernandez, C.I., Gomez-Soria, A., Gonzalez, O., 1997. Chronic intraventricular infusion with NGF improves LTP in old cognitively-impaired rats. Brain Research 770, 1–9.

Bierl, M.A., Isaacson, L.G., 2007. Increased NGF proforms in aged sympathetic neurons and their targets. Neurobiology of Aging 28, 122–34. https://doi.org/10.1016/j.neurobiolaging.2005.11.008

Bierl, M.A., Jones, E.E., Crutcher, K.A., Isaacson, L.G., 2005. “Mature” nerve growth factor is a minor species in most peripheral tissues. Neuroscience Letters 380, 133–7. https://doi.org/10.1016/j.neulet.2005.01.029

Biessels, G.J., Kamal, A., Ramakers, G.M., Urban, I.J., Spruijt, B.M., Erkelens, D.W., Gispen, W.H., 1996. Place learning and hippocampal synaptic plasticity in streptozotocin-induced diabetic rats. Diabetes 45, 1259–66.

Bliss, T.V., Collingridge, G.L., 1993. A synaptic model of memory: long-term potentiation in the hippocampus. Nature 361, 31–9. https://doi.org/10.1038/361031a0

Bradshaw, R.A., Pundavela, J., Biarc, J., Chalkley, R.J., Burlingame, A.L., Hondermarck, H., 2015. NGF and ProNGF: Regulation of neuronal and neoplastic responses through receptor signaling. Advances in biological regulation 58, 16–27. https://doi.org/10.1016/j.jbior.2014.11.003

Bruel-Jungerman, E., Davis, S., Rampon, C., Laroche, S., 2006. Long-term potentiation enhances neurogenesis in the adult dentate gyrus. J Neurosci 26, 5888–93. https://doi.org/10.1523/JNEUROSCI.0782-06.2006

Bruno, Martin A., Cuello, A.C., 2006. Activity-dependent release of precursor nerve growth factor, conversion to mature nerve growth factor, and its degradation by a protease cascade. PNAS 103, 6735–6740. https://doi.org/10.1073/pnas.0510645103

Bruno, M. A., Cuello, A.C., 2006. Activity-dependent release of precursor nerve growth factor, conversion to mature nerve growth factor, and its degradation by a protease cascade. Proc Natl Acad Sci U S A 103, 6735–40.

Can, Ö.D., Üçel, U.İ., Demir Özkay, Ü., Ulupınar, E., 2018. The Effect of Agomelatine Treatment on Diabetes-Induced Cognitive Impairments in Rats: Concomitant

Alterations in the Hippocampal Neuron Numbers. Int J Mol Sci 19. https://doi.org/10.3390/ijms19082461

Chiaretti, A., Conti, G., Falsini, B., Buonsenso, D., Crasti, M., Manni, L., Soligo, M., Fantacci, C., Genovese, O., Calcagni, M.L., Di Giuda, D., Mattoli, M.V., Cocciolillo, F., Ferrara, P., Ruggiero, A., Staccioli, S., Colafati, G.S., Riccardi, R., 2017. Intranasal Nerve Growth Factor administration improves cerebral functions in a child with severe traumatic brain injury: A case report. Brain Injury 31, 1538–1547. https://doi.org/10.1080/02699052.2017.1376760

Cooper-Kuhn, C.M., Winkler, J., Kuhn, H.G., 2004. Decreased neurogenesis after cholinergic forebrain lesion in the adult rat. J Neurosci Res 77, 155–65. https://doi.org/10.1002/jnr.20116

Corvaglia, V., Cilli, D., Scopa, C., Brandi, R., Arisi, I., Malerba, F., La Regina, F., Scardigli, R., Cattaneo, A., 2019. ProNGF is a cell-type specific mitogen for adult hippocampal and for induced neural stem cells. Stem Cells. https://doi.org/10.1002/stem.3037

Cuello, A.C., Bruno, M.A., Allard, S., Leon, W., Iulita, M.F., 2010. Cholinergic involvement in Alzheimer's disease. A link with NGF maturation and degradation. J Mol Neurosci 40, 230–5. https://doi.org/10.1007/s12031-009-9238-z

Dhuria, S.V., Hanson, L.R., Frey, W.H., 2010. Intranasal delivery to the central nervous system: mechanisms and experimental considerations. J Pharm Sci 99, 1654–73. https://doi.org/10.1002/jps.21924

Drever, B.D., Riedel, G., Platt, B., 2011. The cholinergic system and hippocampal plasticity. Behav Brain Res 221, 505–14. https://doi.org/10.1016/j.bbr.2010.11.037

Edwards, R.H., Selby, M.J., Rutter, W.J., 1986. Differential RNA splicing predicts two distinct nerve growth factor precursors. Nature 319, 784–7.

Fahnestock, M., Michalski, B., Xu, B., Coughlin, M.D., 2001. The precursor pro-nerve growth factor is the predominant form of nerve growth factor in brain and is increased in Alzheimer's disease. Mol Cell Neurosci 18, 210–20. https://doi.org/10.1006/mcne.2001.1016

Fahnestock, M., Shekari, A., 2019. ProNGF and Neurodegeneration in Alzheimer's Disease. Frontiers in neuroscience 13, 129. https://doi.org/10.3389/fnins.2019.00129

Frey, I.W., Liu, J., Chen, X.Q., Thorne, R.G., Fawcett, J.R., Ala, T.A., Rahman, Y.E., 1997. Delivery of 125I-NGF to the Brain via the Olfactory Route. Drug delivery 4, 87–92. https://doi.org/10.3109/10717549709051878

Frielingsdorf, H., Simpson, D.R., Thal, L.J., Pizzo, D.P., 2007. Nerve growth factor promotes survival of new neurons in the adult hippocampus. Neurobiol Dis 26, 47–55. https://doi.org/10.1016/j.nbd.2006.11.015

Gibon, J., Barker, P.A., 2017. Neurotrophins and Proneurotrophins: Focus on Synaptic Activity and Plasticity in the Brain. Neuroscientist 23, 587–604. https://doi.org/10.1177/1073858417697037

Guo, J., Wang, J., Zhang, Z., Yan, J., Chen, M., Pang, T., Zhang, L., Liao, H., 2013. proNGF inhibits neurogenesis and induces glial activation in adult mouse dentate gyrus. Neurochem Res 38, 1695–703. https://doi.org/10.1007/s11064-013-1071-7

Hefti, F., Dravid, A., Hartikka, J., 1984. Chronic intraventricular injections of nerve growth factor elevate hippocampal choline acetyltransferase activity in adult rats with partial septo-hippocampal lesions. Brain Res 293, 305–11. https://doi.org/0006-8993(84)91237-X [pii]

Hempstead, B.L., 2014. Deciphering proneurotrophin actions. Handb Exp Pharmacol 220, 17–32. https://doi.org/10.1007/978-3-642-45106-5_2

Ito, S., Ménard, M., Atkinson, T., Brown, L., Whitfield, J., Chakravarthy, B., 2016. Relative expression of the p75 neurotrophin receptor, tyrosine receptor kinase A, and insulin receptor in SH-SY5Y neuroblastoma cells and hippocampi from Alzheimer's disease patients. Neurochem. Int. 101, 22–29. https://doi.org/10.1016/j.neuint.2016.09.015

Iulita, M.F., Cuello, C.A., 2015. The NGF Metabolic Pathway in the CNS and its Dysregulation in Down Syndrome and Alzheimer's disease. Curr Alzheimer Res.

Kelly, A., Conroy, S., Lynch, M.A., 1998. Evidence that nerve growth factor plays a role in long-term potentiation in the rat dentate gyrus. Neuropharmacology 37, 561–70.

Kempermann, G., Jessberger, S., Steiner, B., Kronenberg, G., 2004. Milestones of neuronal development in the adult hippocampus. Trends Neurosci 27, 447–52. https://doi.org/10.1016/j.tins.2004.05.013 S0166-2236(04)00167-5 [pii]

Kempermann, Gerd, Jessberger, S., Steiner, B., Kronenberg, G., 2004. Milestones of neuronal development in the adult hippocampus. Trends Neurosci. 27, 447–452. https://doi.org/10.1016/j.tins.2004.05.013

Kilkenny, C., Browne, W.J., Cuthill, I.C., Emerson, M., Altman, D.G., 2010. Improving bioscience research reporting: the ARRIVE guidelines for reporting animal research. PLoS biology 8, e1000412. https://doi.org/10.1371/journal.pbio.1000412

Knoth, R., Singec, I., Ditter, M., Pantazis, G., Capetian, P., Meyer, R.P., Horvat, V., Volk, B., Kempermann, G., 2010. Murine features of neurogenesis in the human hippocampus across the lifespan from 0 to 100 years. PLoS ONE 5, e8809. https://doi.org/10.1371/journal.pone.0008809

Lee, R., Kermani, P., Teng, K.K., Hempstead, B.L., 2001. Regulation of cell survival by secreted proneurotrophins. Science 294, 1945–8. https://doi.org/10.1126/science.1065057 294/5548/1945 [pii]

Masoudi, R., Ioannou, M.S., Coughlin, M.D., Pagadala, P., Neet, K.E., Clewes, O., Allen, S.J., Dawbarn, D., Fahnestock, M., 2009. Biological activity of nerve growth factor precursor is dependent upon relative levels of its receptors. J Biol Chem 284, 18424–33. https://doi.org/10.1074/jbc.M109.007104

Mohapel, P., Leanza, G., Kokaia, M., Lindvall, O., 2005. Forebrain acetylcholine regulates adult hippocampal neurogenesis and learning. Neurobiology of Aging 26, 939–46. https://doi.org/10.1016/j.neurobiolaging.2004.07.015

Nori, S.L., Rocco, M.L., Florenzano, F., Ciotti, M.T., Aloe, L., Manni, L., 2013. Increased nerve growth factor signaling in sensory neurons of early diabetic rats is corrected by electroacupuncture. Evid Based Complement Alternat Med 2013, 652735. https://doi.org/10.1155/2013/652735

Nykjaer, A., Lee, R., Teng, K.K., Jansen, P., Madsen, P., Nielsen, M.S., Jacobsen, C., Kliemannel, M., Schwarz, E., Willnow, T.E., Hempstead, B.L., Petersen, C.M., 2004. Sortilin is essential for proNGF-induced neuronal cell death. Nature 427, 843–8. https://doi.org/10.1038/nature02319 nature02319 [pii]

Pagadala, P.C., Dvorak, L.A., Neet, K.E., 2006. Construction of a mutated pro-nerve growth factor resistant to degradation and suitable for biophysical and cellular utilization. Proc Natl Acad Sci U S A 103, 17939–43. https://doi.org/0604139103 [pii] 10.1073/pnas.0604139103

Paxinos, G., 1982. The rat brain in stereotaxic coordinates. Academic Press, Sydney.

Pedraza, C.E., Podlesniy, P., Vidal, N., Arevalo, J.C., Lee, R., Hempstead, B., Ferrer, I., Iglesias, M., Espinet, C., 2005. Pro-NGF isolated from the human brain affected by Alzheimer's disease induces neuronal apoptosis mediated by p75NTR. Am J Pathol

166, 533–43. https://doi.org/S0002-9440(10)62275-4 [pii] 10.1016/S0002-9440(10)62275-4

Piotrowski, P., Wierzbicka, K., Smialek, M., 2001. Neuronal death in the rat hippocampus in experimental diabetes and cerebral ischaemia treated with antioxidants. Folia Neuropathol 39, 147–54.

Protto, V., Soligo, M., De Stefano, M.E., Farioli-Vecchioli, S., Marlier, L., Nistico, R., Manni, L., 2019. Electroacupuncture in rats normalizes the diabetes-induced alterations in the septo-hippocampal cholinergic system. Hippocampus. https://doi.org/10.1002/hipo.23088

Reisi, P., Babri, S., Alaei, H., Sharifi, M.R., Mohaddes, G., Noorbakhsh, S.M., Lashgari, R., 2010. Treadmill running improves long-term potentiation (LTP) defects in streptozotocin-induced diabetes at dentate gyrus in rats. Pathophysiology : the official journal of the International Society for Pathophysiology / ISP 17, 33–8. https://doi.org/10.1016/j.pathophys.2009.06.001

Riudavets, M.A., Iacono, D., Resnick, S.M., O'Brien, R., Zonderman, A.B., Martin, L.J., Rudow, G., Pletnikova, O., Troncoso, J.C., 2007. Resistance to Alzheimer's pathology is associated with nuclear hypertrophy in neurons. Neurobiol. Aging 28, 1484–1492. https://doi.org/10.1016/j.neurobiolaging.2007.05.005

Rocco, M.L., Pristera, A., Pistillo, L., Aloe, L., Canu, N., Manni, L., 2013. Brain Cholinergic Markers and Tau Phosphorylation are Altered in Experimental Type 1 Diabetes: Normalization by Electroacupuncture. J Alzheimers Dis 33, 767–73.

Schliebs, R., Arendt, T., 2011. The cholinergic system in aging and neuronal degeneration. Behav Brain Res 221, 555–63. https://doi.org/10.1016/j.bbr.2010.11.058

Seidah, N.G., Benjannet, S., Pareek, S., Savaria, D., Hamelin, J., Goulet, B., Laliberte, J., Lazure, C., Chretien, M., Murphy, R.A., 1996. Cellular processing of the nerve growth factor precursor by the mammalian pro-protein convertases. Biochem J 314 (Pt 3), 951–60.

Selby, M.J., Edwards, R., Sharp, F., Rutter, W.J., 1987. Mouse nerve growth factor gene: structure and expression. Mol Cell Biol 7, 3057–64.

Sherin, A., Anu, J., Peeyush, K.T., Smijin, S., Anitha, M., Roshni, B.T., Paulose, C.S., 2012. Cholinergic and GABAergic receptor functional deficit in the hippocampus of insulin-induced hypoglycemic and streptozotocin-induced diabetic rats. Neuroscience 202, 69–76. https://doi.org/10.1016/j.neuroscience.2011.11.058

Snyder, J.S., Kee, N., Wojtowicz, J.M., 2001. Effects of adult neurogenesis on synaptic plasticity in the rat dentate gyrus. J Neurophysiol 85, 2423–31.

Soligo, M., Albini, M., Bertoli, F.L., Marzano, V., Protto, V., Bracci-Laudiero, L., Minnone, G., De Benedetti, F., Chiaretti, A., Mantuano, E., Manni, L., 2019. Different responses of PC12cells to different pro-nerve growth factor protein variants. Neurochem Int 104498. https://doi.org/10.1016/j.neuint.2019.104498

Soligo, M., Piccinin, S., Protto, V., Gelfo, F., De Stefano, M.E., Florenzano, F., Berretta, E., Petrosini, L., Nistico, R., Manni, L., 2017. Recovery of hippocampal functions and modulation of muscarinic response by electroacupuncture in young diabetic rats. Scientific reports 7, 9077. https://doi.org/10.1038/s41598-017-08556-z

Soligo, M., Protto, V., Florenzano, F., Bracci-Laudiero, L., De Benedetti, F., Chiaretti, A., Manni, L., 2015. The mature/pro nerve growth factor ratio is decreased in the brain of diabetic rats: Analysis by ELISA methods. Brain Research 1624, 455–68. https://doi.org/10.1016/j.brainres.2015.08.005

Teles-Grilo Ruivo, L.M., Mellor, J.R., 2013. Cholinergic modulation of hippocampal network function. Frontiers in synaptic neuroscience 5, 2. https://doi.org/10.3389/fnsyn.2013.00002

Thoenen, H., Zafra, F., Hengerer, B., Lindholm, D., 1991. The synthesis of nerve growth factor and brain-derived neurotrophic factor in hippocampal and cortical neurons is regulated by specific transmitter systems. Annals of the New York Academy of Sciences 640, 86–90.

Thorne, R.G., Frey, W.H., 2001. Delivery of neurotrophic factors to the central nervous system: pharmacokinetic considerations. Clin Pharmacokinet 40, 907–46.

Tiveron, C., Fasulo, L., Capsoni, S., Malerba, F., Marinelli, S., Paoletti, F., Piccinin, S., Scardigli, R., Amato, G., Brandi, R., Capelli, P., D'Aguanno, S., Florenzano, F., La Regina, F., Lecci, A., Manca, A., Meli, G., Pistillo, L., Berretta, N., Nistico, R., Pavone, F., Cattaneo, A., 2013. ProNGF\NGF imbalance triggers learning and memory deficits, neurodegeneration and spontaneous epileptic-like discharges in transgenic mice. Cell Death Differ 20, 1017–30. https://doi.org/10.1038/cdd.2013.22

Uzakov, S.S., Ivanov, A.D., Salozhin, S.V., Markevich, V.A., Gulyaeva, N.V., 2015. Lentiviral-mediated overexpression of nerve growth factor (NGF) prevents beta-amyloid [25-35]-induced long term potentiation (LTP) decline in the rat hippocampus. Brain Research. https://doi.org/10.1016/j.brainres.2015.07.051

Van der Borght, K., Mulder, J., Keijser, J.N., Eggen, B.J., Luiten, P.G., Van der Zee, E.A., 2005. Input from the medial septum regulates adult hippocampal neurogenesis. Brain Res Bull 67, 117–25. https://doi.org/10.1016/j.brainresbull.2005.06.018

Welsh, B., Wecker, L., 1991. Effects of streptozotocin-induced diabetes on acetylcholine metabolism in rat brain. Neurochem Res 16, 453–60.

Wilson, G.L., Leiter, E.H., 1990. Streptozotocin interactions with pancreatic beta cells and the induction of insulin-dependent diabetes. Curr Top Microbiol Immunol 156, 27–54.

Wright, B.J., Jackson, M.B., 2014. Long-term potentiation in hilar circuitry modulates gating by the dentate gyrus. J. Neurosci. 34, 9743–9753. https://doi.org/10.1523/JNEUROSCI.0814-14.2014

Zafra, F., Castren, E., Thoenen, H., Lindholm, D., 1991. Interplay between glutamate and gamma-aminobutyric acid transmitter systems in the physiological regulation of brain-derived neurotrophic factor and nerve growth factor synthesis in hippocampal neurons. Proc Natl Acad Sci U S A 88, 10037–41.

Zhao, Y., Shen, Z., Zhang, D., Luo, H., Chen, J., Sun, Y., Xiao, Q., 2017. Ghrelin ameliorates nerve growth factor Dysmetabolism and inflammation in STZ-induced diabetic rats. Metab Brain Dis 32, 903–912. https://doi.org/10.1007/s11011-017-0001-9

Figure legends

Figure 1. proNGF-A and proNGF-B affect long term potentiation in dentate gyrus. Long-term potentiation at perforant-pathway (DG-LTP) was measured in healthy (**A**) and diabetic (**B**) rats intranasally treated with saline, proNGF-A or proNGF-B. Field excitatory postsynaptic potentials (fEPSP) were recorded and expressed as the percentage of the pre-tetanus baseline (**A-B**). Changes in fEPSP slopes before and 60 min after the induction of LTP by high-frequency stimulation (HFS) of the medial perforant pathway (black arrows) are shown. The insets represent typical fEPSP recordings; calibration bars: 0.5 mV, 10 ms. The DG-LTP magnitude 50-60 minutes after HFS relating to healthy and diabetic animals respectively (indicated with black boxes in panels **A** and **B**) is reported in panel **C**. The details of two-way ANOVA performed on data presented in panel **C**, and the significant multiple comparisons relative to disease induction (healthy vs diabetic, not reported in panel **C**), are depicted in panels **D** and **E** respectively. Data are presented as means ± SEM (n=8 for each experimental group) and two-way ANOVA (**D**) was followed by Bonferroni multiple comparison (**C, E**).

Figure 2. proNGF protein variants affect hippocampal cell number and morphology. (**A-B**) Representative images of DG-Hilus and DG-Granular layer of healthy and diabetic rats treated with saline, proNGF-A or proNGF-B after Hoechst nuclear staining. (**C, F**) Quantitative analysis of the total number of cells in DG-Hilus and DG-Granular layer, respectively. (**D, G**) Quantitative analysis of the nuclear size of DG-Hilus and DG-Granular layer, respectively. (**E, H**) Quantitative analysis of the total number of $NeuN^+$ cells in DG-Hilus and DG-Granular layer, respectively. Data are presented as means ± SEM and two-way ANOVA (reported below each graph) was followed by Bonferroni multiple comparisons. The P values reported in the graphs refer to the multiple comparison between pharmacological treatments within the experimental group of healthy or diabetic

animals. The tables (below the graphs) show P values of the multiple comparison between healthy and diabetic rats within the same treatment group (n=8 hippocampi for each experimental group).

Figure 3. proNGF-B impairs hippocampal neurogenesis and proNGF-A rescues the terminal differentiation of neuronal progenitors. (**A**) Immunolocalization of BrdU (green) in DG of healthy and diabetic rats intranasally treated with saline, proNGF-A or proNGF-B. The insets represent the enlargement (zoom: 7X) of the arrow-pointed cells. (**B**) Quantitative analysis of the number of BrdU-immunopositive ($BrdU^+$) cells in hippocampal-DG. (**C**) Representative image of the immunolocalization of BrdU, doublecortin (DCX) and NeuN in hippocampal DG. The insets represent the arrow-pointed co-labeled $BrdU^+/DCX^+$ and $BrdU^+/NeuN^+$ cells, respectively (zoom: 9X). Quantitative analysis of the number of double immunopositive $BrdU^+/DCX^+$ (**D**) or $BrdU^+/NeuN^+$ cells (**E**). Data are presented as means ± SEM and two-way ANOVA (reported below the graphs) was followed by Bonferroni multiple comparisons. The P values reported in the graphs refer to the multiple comparisons between pharmacological treatments within the experimental group of healthy or diabetic animals. The tables (below the graphs) show P values of the multiple comparisons between healthy and diabetic rats within the same treatment group (n=6 hippocampi for each experimental group).

Figure 4. proNGF protein variants affect hippocampal cell proliferation. (**A**) Immunolocalization of ki67 (red) and nuclei (blue) in DG of healthy and diabetic rats intranasally delivered with saline, proNGF-A or proNGF-B. The insets represent the enlargement (zoom: 5X) of cells in the white boxes. (**B**) Quantification of ki67-immunopositive ($ki67^+$) cells number in hippocampal-DG. (**C**) Representative picture of the immunolocalization of ki67 (red), DCX (green) and nuclei (blue) in DG. (**D**) Quantification of the number of double immunopositive $ki67^+/DCX^+$ cells in DG of healthy

and diabetic rats. Data are presented as means ± SEM and two-way ANOVA (reported below the graphs) was followed by Bonferroni multiple comparisons. The P values reported in the graphs refer to multiple comparisons between pharmacological treatments within the experimental groups of healthy or diabetic animals. The tables (below the graphs) show P values of the multiple comparisons between healthy and diabetic rats within the same treatment group (n=6 hippocampi for each experimental group).

Figure 5. proNGFs modulate the medial septum cholinergic phenotype. (**A**) graphical sketch representing cholinergic neurons in the medial septum (MS) and cholinergic fimbria fibers projecting to hippocampal dentate gyrus (DG). Black boxes indicate the area where the quantitative analysis was performed. (**B**) Quantification of the total $NeuN^+$ cells/0.6 mm^2 in MS of healthy and diabetic rats treated with saline, proNGF-A or proNGF-B. (**C**) Representative images of $ChAT^+$ cells in the MS. (**D**) Quantification of the number of $ChAT^+$ cells/0.6 mm^2 in the MS. (**E**) Quantification of ChAT content in cholinergic cells. Data are presented as means ± SEM and two-way ANOVA (reported below the graphs) was followed by Bonferroni multiple comparisons. The P values reported in the graphs refer to the multiple comparison between pharmacological treatments within the experimental group of healthy or diabetic animals. The tables (below the graphs) show P values of the multiple comparisons between healthy and diabetic rats within the same treatment group (n=4 rats for each experimental group).

Figure 6. proNGFs modulate the septo-hippocampal cholinergic fibers. (**A**) graphical sketch representing cholinergic neurons in the medial septum (MS) and cholinergic fimbria fibers projecting to hippocampal dentate gyrus (DG). Black boxes indicate the areas where the quantitative analysis was performed. (**B**) Representative images of $ChAT^+$ fimbria fibers in a region proximal to MS in healthy and diabetic rats treated with saline, proNGF-A or proNGF-B. (**C**) Quantification of the percentage of area covered by $ChAT^+$ fimbria fibers

proximal to MS. (**D**) Quantification of ChAT content in cholinergic fibers proximal to MS. (**E**) Representative images of $ChAT^{+}$ fimbria fibers at the hippocampus entrance. (**F**) Quantification of the percentage of area covered by ChAT immunostaining at the hippocampus entrance. (**G**) Quantification of ChAT content in cholinergic fibers at the hippocampus entrance. Data are presented as means ± SEM and two-way ANOVA (reported below each graph) was followed by Bonferroni multiple comparisons. The P values reported in the graphs refer to the multiple comparison between pharmacological treatments within the experimental group of healthy or diabetic animals. The tables (below the graphs) show P values of the multiple comparison between healthy and diabetic rats within the same treatment group (n=4 rats for each experimental group).

A

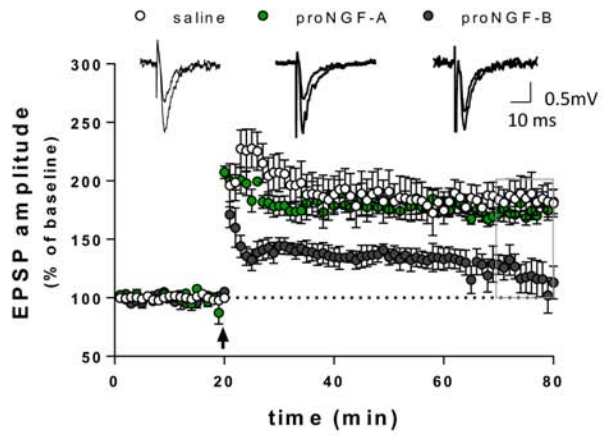

B

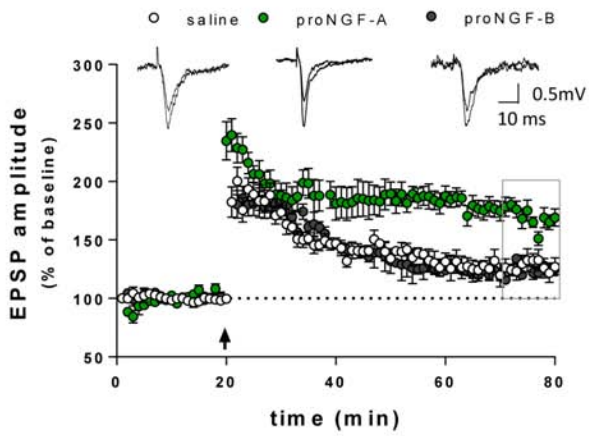

C

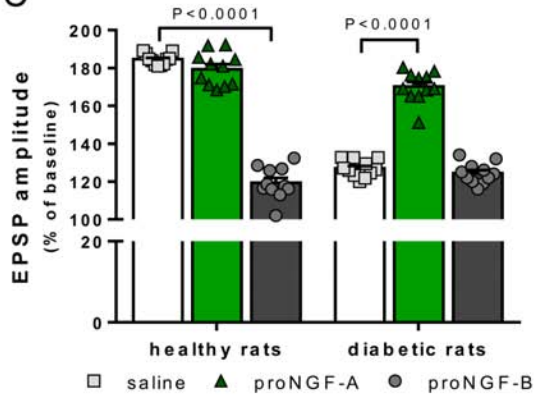

D

Disease	$F_{(1, 60)}$=154.2; P<0.0001
Treatment	$F_{(2, 60)}$=348.0; P<0.0001
Disease x Treatment	$F_{(2, 60)}$=130.5; P<0.0001

E

healthy rats *vs* diabetic rats	
saline-treatment	P< 0.0001
proNGF-A-treatment	P=0.0066

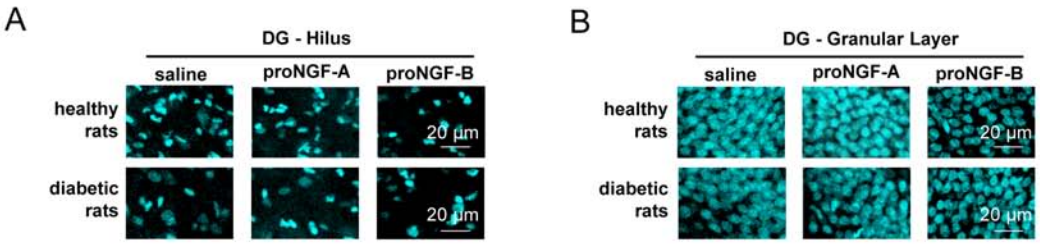

DG - Hilus

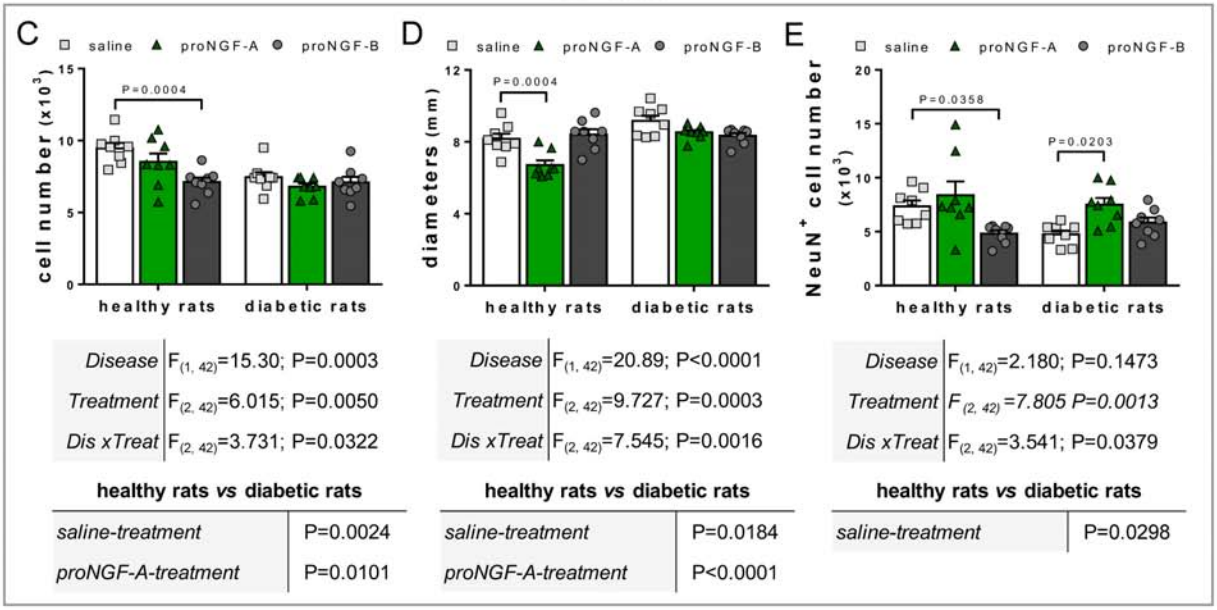

	C	D	E
Disease	$F_{(1, 42)}$=15.30; P=0.0003	$F_{(1, 42)}$=20.89; P<0.0001	$F_{(1, 42)}$=2.180; P=0.1473
Treatment	$F_{(2, 42)}$=6.015; P=0.0050	$F_{(2, 42)}$=9.727; P=0.0003	$F_{(2, 42)}$=7.805 P=0.0013
Dis xTreat	$F_{(2, 42)}$=3.731; P=0.0322	$F_{(2, 42)}$=7.545; P=0.0016	$F_{(2, 42)}$=3.541; P=0.0379

healthy rats *vs* diabetic rats					
saline-treatment	P=0.0024	*saline-treatment*	P=0.0184	*saline-treatment*	P=0.0298
proNGF-A-treatment	P=0.0101	*proNGF-A-treatment*	P<0.0001		

DG - Granular Layer

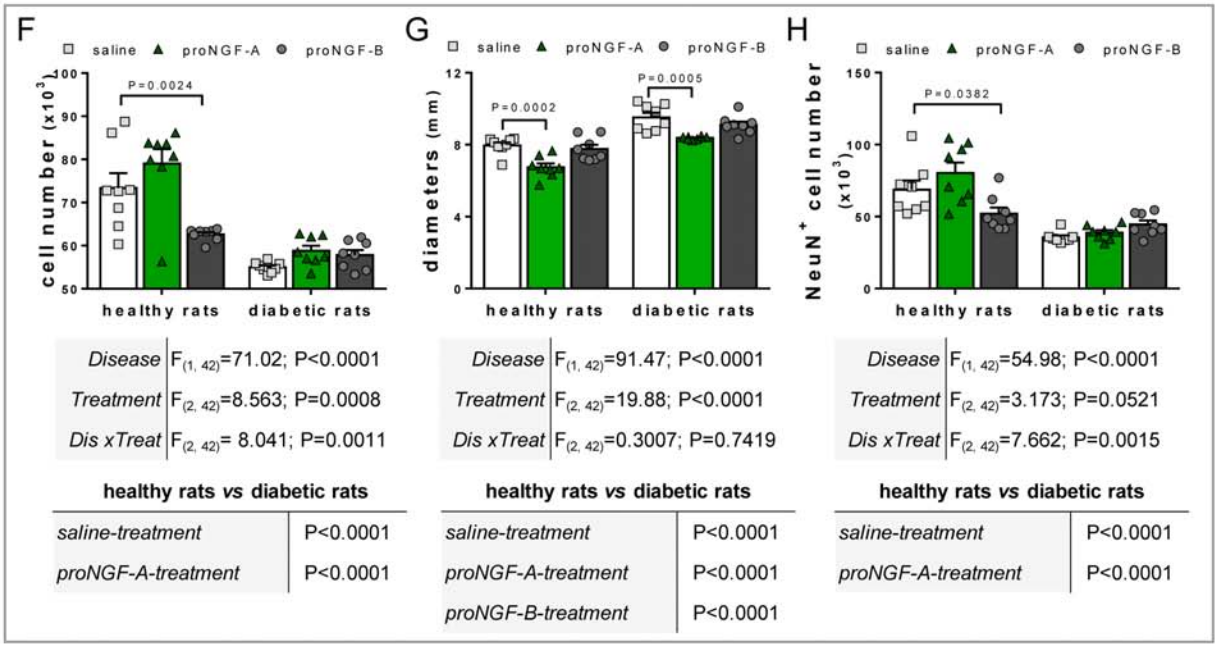

	F	G	H
Disease	$F_{(1, 42)}$=71.02; P<0.0001	$F_{(1, 42)}$=91.47; P<0.0001	$F_{(1, 42)}$=54.98; P<0.0001
Treatment	$F_{(2, 42)}$=8.563; P=0.0008	$F_{(2, 42)}$=19.88; P<0.0001	$F_{(2, 42)}$=3.173; P=0.0521
Dis xTreat	$F_{(2, 42)}$= 8.041; P=0.0011	$F_{(2, 42)}$=0.3007; P=0.7419	$F_{(2, 42)}$=7.662; P=0.0015

healthy rats *vs* diabetic rats					
saline-treatment	P<0.0001	*saline-treatment*	P<0.0001	*saline-treatment*	P<0.0001
proNGF-A-treatment	P<0.0001	*proNGF-A-treatment*	P<0.0001	*proNGF-A-treatment*	P<0.0001
		proNGF-B-treatment	P<0.0001		

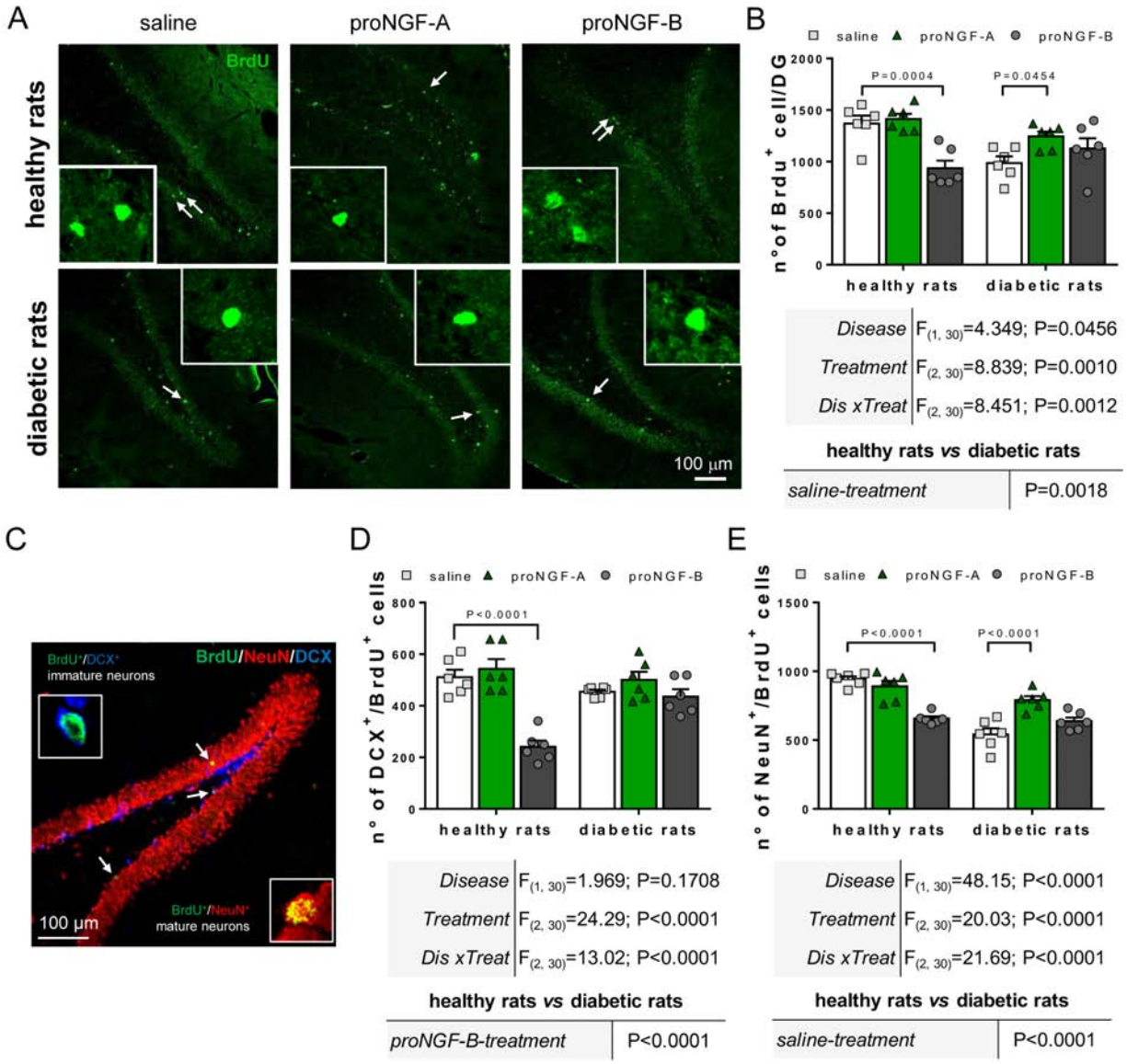
A
saline
proNGF-A
proNGF-B
healthy rats
diabetic rats
BrdU
100 µm
B
saline
proNGF-A
proNGF-B
n°of Brdu+ cell/DG
P=0.0004
P=0.0454
healthy rats
diabetic rats
Disease F(1, 30)=4.349; P=0.0456
Treatment F(2, 30)=8.839; P=0.0010
Dis xTreat F(2, 30)=8.451; P=0.0012
healthy rats vs diabetic rats
saline-treatment P=0.0018
C
BrdU+/DCX+
immature neurons
BrdU/NeuN/DCX
BrdU+/NeuN+
mature neurons
100 µm
D
saline
proNGF-A
proNGF-B
n° of DCX+/BrdU+ cells
P<0.0001
healthy rats
diabetic rats
Disease F(1, 30)=1.969; P=0.1708
Treatment F(2, 30)=24.29; P<0.0001
Dis xTreat F(2, 30)=13.02; P<0.0001
healthy rats vs diabetic rats
proNGF-B-treatment P<0.0001
E
saline
proNGF-A
proNGF-B
n° of NeuN+/BrdU+ cells
P<0.0001
P<0.0001
healthy rats
diabetic rats
Disease F(1, 30)=48.15; P<0.0001
Treatment F(2, 30)=20.03; P<0.0001
Dis xTreat F(2, 30)=21.69; P<0.0001
healthy rats vs diabetic rats
saline-treatment P<0.0001

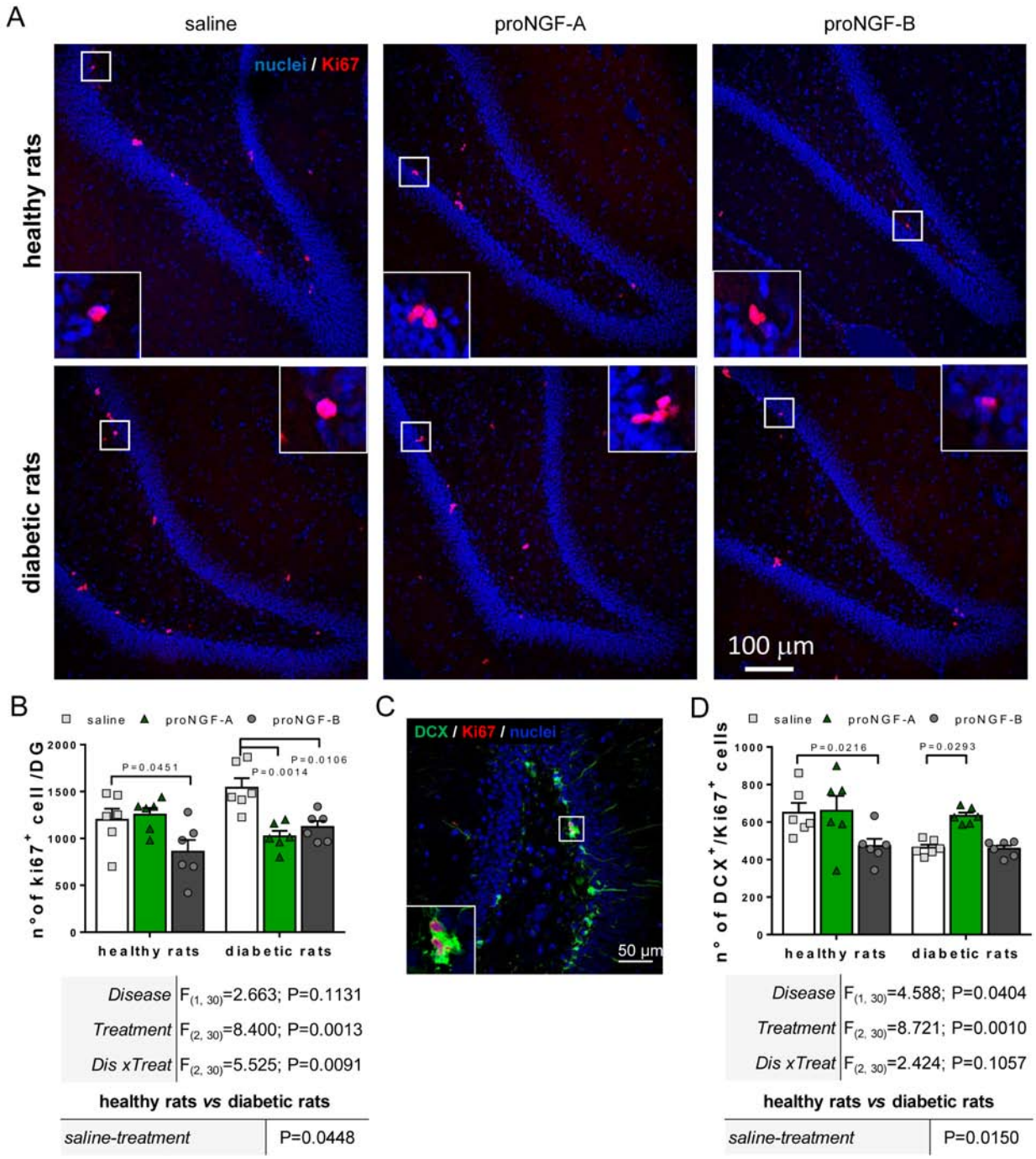

Disease	$F_{(1, 30)}$=2.663; P=0.1131
Treatment	$F_{(2, 30)}$=8.400; P=0.0013
Dis xTreat	$F_{(2, 30)}$=5.525; P=0.0091

healthy rats *vs* diabetic rats

saline-treatment	P=0.0448

Disease	$F_{(1, 30)}$=4.588; P=0.0404
Treatment	$F_{(2, 30)}$=8.721; P=0.0010
Dis xTreat	$F_{(2, 30)}$=2.424; P=0.1057

healthy rats *vs* diabetic rats

saline-treatment	P=0.0150

A

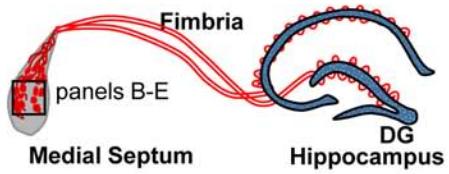

B

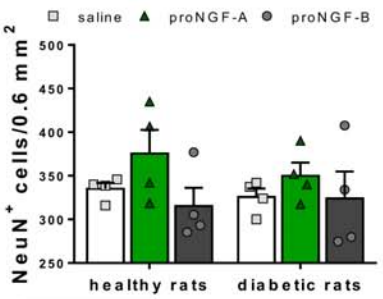

Disease	$F_{(1, 18)}$=0.2760; P=0.6057
Treatment	$F_{(2, 18)}$=2.4050; P=0.1187
Dis xTreat	$F_{(2, 18)}$=0.3543; P=0.7064

C

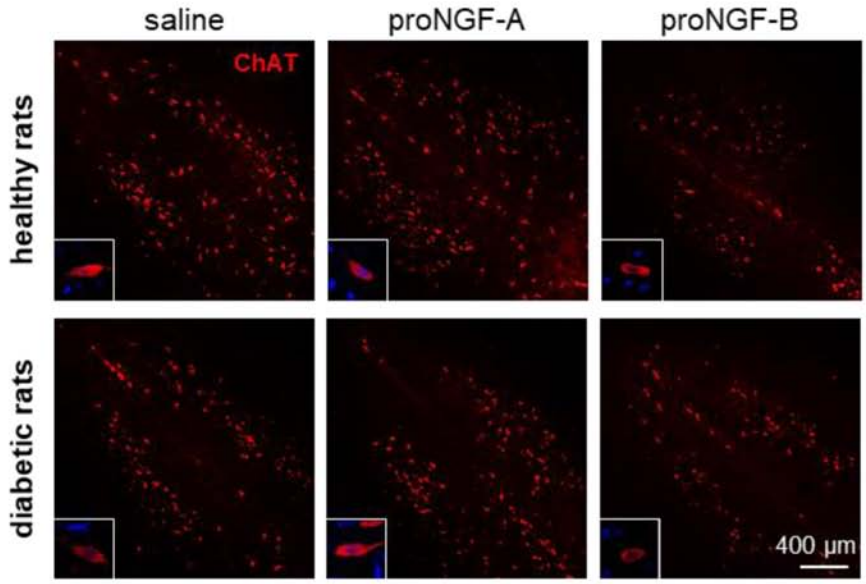

D

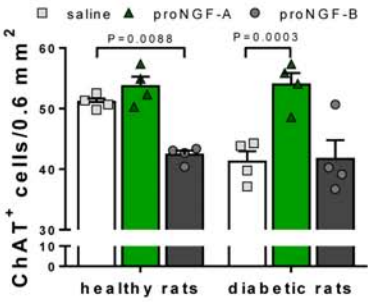

Disease	$F_{(1, 18)}$=5.518; P=0.0304
Treatment	$F_{(2, 18)}$=22.39; P<0.0001
Dis xTreat	$F_{(2, 18)}$=4.855; P=0.0206

healthy rats *vs* diabetic rats

saline-treatment	P=0.0032

E

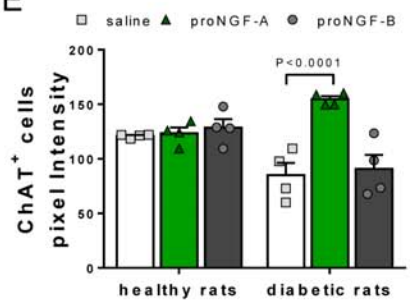

Disease	$F_{(1, 18)}$=4.708; P=0.0436
Treatment	$F_{(2, 18)}$=11.36; P=0.0006
Dis xTreat	$F_{(2, 18)}$=11.93; P=0.0005

healthy rats *vs* diabetic rats

saline-treatment	P=0.0161
proNGF-A-treatment	P=0.0409
proNGF-B-treatment	P=0.0112

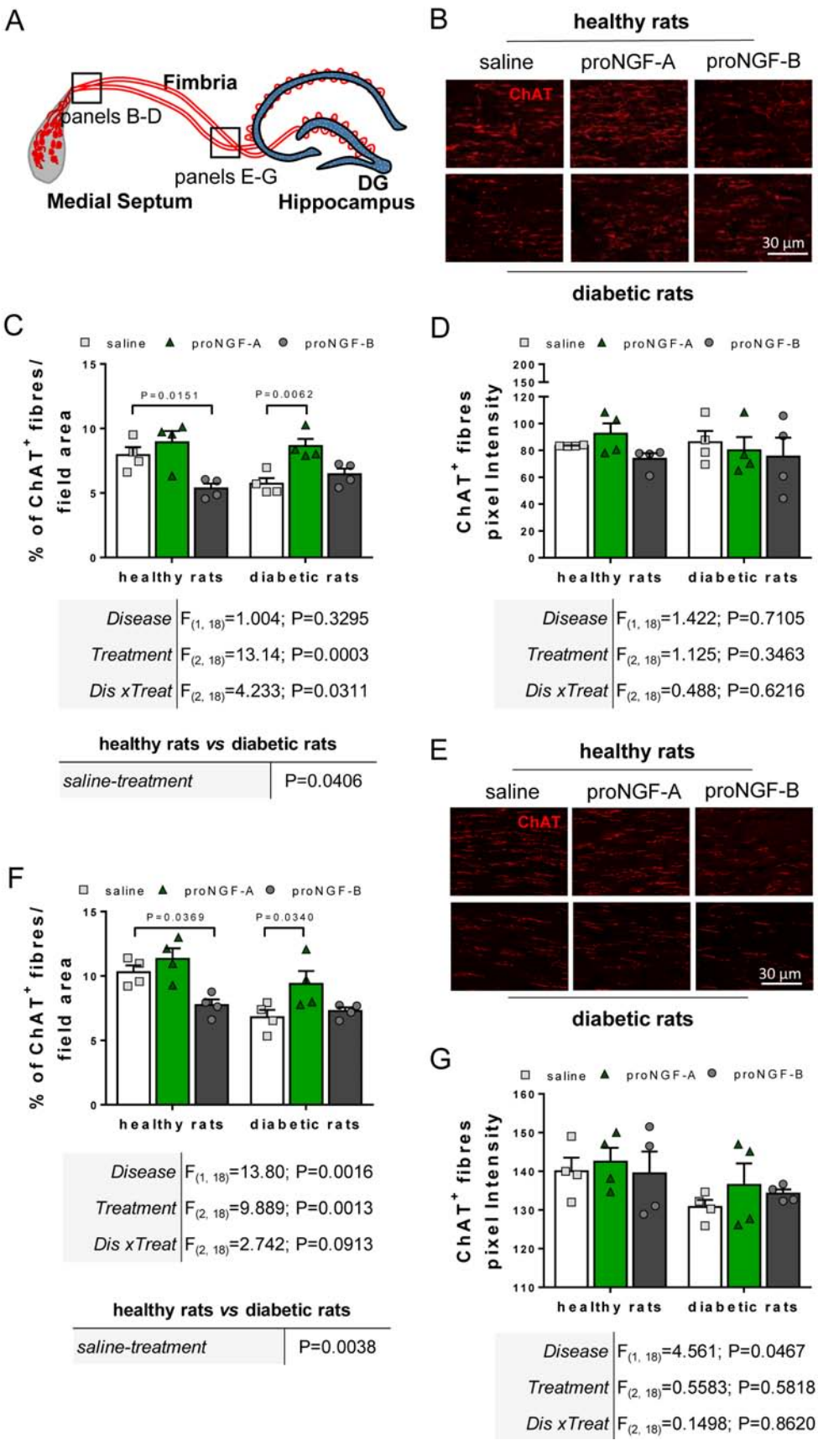
A
Fimbria
panels B-D
panels E-G
Medial Septum
DG
Hippocampus
B
healthy rats
saline
proNGF-A
proNGF-B
ChAT
30 µm
diabetic rats
C
saline
proNGF-A
proNGF-B
% of ChAT+ fibres/ field area
P=0.0151
P=0.0062
healthy rats
diabetic rats
Disease F(1, 18)=1.004; P=0.3295
Treatment F(2, 18)=13.14; P=0.0003
Dis xTreat F(2, 18)=4.233; P=0.0311
healthy rats vs diabetic rats
saline-treatment P=0.0406
D
saline
proNGF-A
proNGF-B
ChAT+ fibres pixel Intensity
healthy rats
diabetic rats
Disease F(1, 18)=1.422; P=0.7105
Treatment F(2, 18)=1.125; P=0.3463
Dis xTreat F(2, 18)=0.488; P=0.6216
E
healthy rats
saline
proNGF-A
proNGF-B
ChAT
30 µm
diabetic rats
F
saline
proNGF-A
proNGF-B
% of ChAT+ fibres/ field area
P=0.0369
P=0.0340
healthy rats
diabetic rats
Disease F(1, 18)=13.80; P=0.0016
Treatment F(2, 18)=9.889; P=0.0013
Dis xTreat F(2, 18)=2.742; P=0.0913
healthy rats vs diabetic rats
saline-treatment P=0.0038
G
saline
proNGF-A
proNGF-B
ChAT+ fibres pixel Intensity
healthy rats
diabetic rats
Disease F(1, 18)=4.561; P=0.0467
Treatment F(2, 18)=0.5583; P=0.5818
Dis xTreat F(2, 18)=0.1498; P=0.8620

Effects of intranasally-delivered pro-nerve growth factors on the septo-hippocampal system in healthy and diabetic rats

Marzia Soligo[1], Virginia Protto[1], Antonio Chiaretti[2], Sonia Piccinin[3], Maria Egle De Stefano[4], Robert Nisticò[3,5], Luisa Bracci-Laudiero[1,6], Luigi Manni[1].

[1] *Institute of Translational Pharmacology, Consiglio Nazionale Delle Ricerche (CNR), Rome, Italy*

[2] *Institute of Pediatrics, Università Cattolica del Sacro Cuore, Rome – Italy*

[3] *European Brain Research Institute (EBRI), Rome, Italy*

[4] *Department of Biology and Biotechnology "Charles Darwin", Sapienza University, Rome, Italy*

[5] *Department of Biology, University of Rome Tor Vergata, Rome, Italy*

[6] *Division of Rheumatology and Immuno-Rheumatology Research Laboratories, Bambino Gesù Children's Hospital, Rome, Italy*

HIGHLIGHTS

- Native mouse proNGF-A/-B were delivered to the rat brain via intranasal route
- proNGF-A improves DG-LTP and SGZ-neurogenesis in rat with diabetic encephalopathy
- proNGF-A rescues the diabetes-impaired cholinergic phenotype in the medial septum
- proNGF-B depress DG-LTP and impairs SGZ-neurogenesis in healthy rats
- proNGF-B impairs cholinergic phenotype and neurotransmission in healthy rats